

Dear Editor,

In response to the comments made by the reviewers, we have substantially improved the presentation of the paper. In particular, we have made the following changes to the manuscript:

1. The abstract now states some key numerical results (previously it had been worded in a mostly qualitative way).
2. The introduction is now much expanded, containing a more exhaustive discussion of the literature.
3. We corrected a minor error with the temperature climatology: Data above 25 km were actually not MOPI measurements, they were reanalyses and other data as used for retrieval of ozone from MOPI measurements.
4. The description of the model has been expanded, addressing several of the reviewers' comments.
5. We now state regression fits to every pair of the SCO,  $j(\text{O1D})$ , and OH variables displayed in fig. 4.
6. We have expanded the Conclusions section, now charting a way forward how this study could be of use in the future to address problems with simulating OH in global models.
7. The figures have been overhauled. We now consistently use the blue-red scale, with white reserved for the 0 value (if present).

We hope the paper is now suitable for publication in ACP, and are looking forward to hearing from you.

Best regards,



Olaf Morgenstern (on behalf of all co-authors).

# ***Interactive comment on “Assessing the sensitivity of the hydroxyl radical to model biases in composition and temperature using a single-column photochemical model for Lauder, New Zealand” by L. López-Comí et al.***

**L. López-Comí et al.**

olaf.morgenstern@niwa.co.nz

Received and published: 3 October 2016

We thank the reviewer for his/her thoughtful comments. The reviewer's comments are repeated below in italics.

*The authors report a study of the effects on OH of constraining model calculations to observations of ozone photolysis rates and concentrations of ozone, water vapour, CO and methane, as opposed to model derived fields for these variables. The model used is a single column photochemical model, based on the NIWA-UKCA model, and enables a focus on the model chemistry owing to removal of transport and physical*

Printer-friendly version

Discussion paper



*processes whilst also demonstrating changes in chemical effects on OH as a function of altitude.*

*My major comment with the paper regards a lack of detail, and insufficient attention given to the wider applicability of the results obtained in Lauder, New Zealand, to global chemistry-climate modelling.*

We are now providing significantly more detail, improving the presentation of the results, and have also expanded the conclusions section in response to the reviewer's concern about insufficient coverage of the wider significance of the research.

1. *Abstract: The general trends for changes in OH are described but these should be quantified throughout.*

We have modified the abstract trying to strike a balance between giving some quantitative information and not overloading it with numbers which can make the abstract unreadable. This was also in response to a comment by the 2nd reviewer.

2. *Introduction: The introduction is rather short and lacking in detail. The rationale for studying OH is brief, and the paper would benefit from an expanded discussion of why it is such an important model target. The statement that 'considerable disagreement among . . . models' should be quantified, and given that the abstract describes the possibility of this work explaining 'differences in simulated OH between global chemistry models and relative to observations' some discussion of relevant previous studies is warranted. Differences in model outputs observed in intercomparisons such as ACCMIP could be of interest here, and would help place this paper and its results in greater context of previous work.*

We have now considerably expanded the introduction, giving quantitative information on the disagreement e.g. found in ACCMIP models. We hope that this addresses the reviewer's concern.

[Printer-friendly version](#)[Discussion paper](#)

3. *The Emmerson et al. papers referenced (line 47) refer to box models, some reference to single-column models, and examples of their use, should be given. There is no reference given for Lauder being 'known for its clean air' (line 49), or much detail given the 'large diversity of available measurements' (line 50). Apart from O<sub>3</sub>, H<sub>2</sub>O, CO, and CH<sub>4</sub>, what species are measured? Are there measurements of NO<sub>x</sub> (what are the average values?) or other VOCs?*

References to single-column models have been added in the text, as well as their different applications. Single-column models for OH chemistry, other than our own, to our understanding do not exist. The paper now states that the Emmerson et al. papers refer to the development and application of box models, rather than SCMs. See paragraph 4 of the introduction.

A reference attributing Lauder to be a clean air site has been added.

In addition to the measurements used here, Lauder produces measurements of total-column NO<sub>2</sub>, total-column BrO, and FTS measurements of a variety of species (mostly as total columns) that are reported at NDACC. For this study, relatively high-resolution profile information is needed which in the troposphere is only achieved by the ozone sondes (which produce O<sub>3</sub>, H<sub>2</sub>O, and *T* profiles). Near-surface NO<sub>2</sub> has only been measured episodically at Lauder; its abundance has generally been at or near the detection limit. We don't know what the averages would be. These measurements are unsuitable to constrain the SCM with. Lauder is well known for its total-column NO<sub>2</sub> measurements but these are dominated by a stratospheric contribution and cannot be used to infer tropospheric abundances of NO<sub>2</sub>.

A few VOCs have been derived as total-columns from FTS measurements (C<sub>2</sub>H<sub>6</sub>, HCHO, HCN, CH<sub>3</sub>OH). These species are all orders of magnitude less abundant than CH<sub>4</sub>, and biases in them would have a small direct impact on OH. For HCHO, there is a considerable discrepancy between modelled and measured total columns, which we cannot fully explain (Zeng et al., 2015) and which may

[Printer-friendly version](#)[Discussion paper](#)

be indicative of a knowledge gap regarding VOCs at Lauder. A more exhaustive discussion of this is however beyond the scope of this paper.

4. *Line 173: Please clarify that the changes in modelled  $O_3$  (Fig. 2a) are a result of constraining to the observations and not a model result. Is there any explanation for the increases in spring and decreases in autumn compared to the reference simulation? Or for the altitude dependence?*

In subsection 3.1 (OH sensitivity to  $O_3$  biases), paragraph 2, we now clarify that the  $O_3$  difference (fig. 2a) is indeed NIWA-UKCA ozone versus ozonesonde data. The caption of fig. 2a is also changed accordingly.

Exploring the causes of the ozone and temperature biases in NIWA-UKCA is the subject of an ongoing investigation; we don't fully understand why these biases occur either. Exploring these causes is beyond the scope of this paper; here we focus only on the consequences of these biases for OH.

5. *Line 181: Is the 5% increase an average value over all altitudes/seasons? Please clarify.*

We now clarify that this pertains only to the spring season and the altitude range of 2-6 km. 5% is about the maximum difference.

6. *Line 185: The statement that the increases in OH are the result of increases in  $j_{O1D}$  seems rather obvious given that this is the only parameter that has been changed.*

We have rephrased this sentence. Indeed there is no surprise here, but we have gained a simple quantification of the impact of TCO errors on OH.

7. *Line 188: Please explain (and discuss) more clearly what you mean by the statement that the magnitudes of the kinetics and photolysis effects are comparable. Figures 2c and 2d show the changes to  $j_{O1D}$  and OH respectively, how do these*

[Printer-friendly version](#)[Discussion paper](#)

*suggest anything about the  $O_3$  bias? The values shown in Figures 2a and 2b, which do correspond to the kinetics effects, are not comparable or similar to those in Figures 2c and 2d.*

The text now makes this clearer. Indeed the patterns are different, but the ranges of values are comparable.

8. *Line 193: What is the significance of a near exponential relationship? Does it have a physical basis? From the plot it is not clear that there is a near exponential relationship, if there is and it is significant, please show it on the plot and give the parameters describing the relationship. Does Figure 3 show data from all altitudes? The discussion comments on an altitude of 6 km, how does this relate to the data shown in the figure?*

The near-exponential is motivated by the Lambert-Beer Law, which links attenuation to optical thickness. The finding is still semi-empirical because the solar UV light is not monochromatic and the optical thickness of ozone is wavelength dependent. The plot only shows how OH would respond to a systematic change of the SCO. We now provide empirical fits in all three panels. In the case of SCO versus  $j_{O1D}$ , we account for the curvature by fitting a parabola to  $\log j_{O1D}$ . The fit parameters are stated in the panels, and some text is added to this effect.

9. *Line 199: Again, explain the significance of the exponential relationship and give the parameters describing it.*

The same as above.

10. *Line 213: The percentages given in the discussion are given as fractions in the figures, please change one or the other for consistency.*

We have changed the text to make it consistent with the panels.

11. *Line 235: What is the fraction of the total OH loss to  $CH_4$  and CO in the model? It is not clear from the discussion what fraction of the total OH loss occurs due*

Printer-friendly version

Discussion paper



to reactions with  $\text{CH}_4$  and  $\text{CO}$ , what are the implications of the presence of other species, and thus the applicability of the results obtained in this work to more polluted regions. The  $\text{OH}$  concentrations shown in Figure 3 seem particularly high.

Unfortunately we cannot straightforwardly diagnose in the SCM what the fraction of  $\text{OH}$  lost to  $\text{CH}_4$  or  $\text{CO}$  is. For NIWA-UKCA, such diagnoses exist for the global domain. In the troposphere,  $\text{OH} + \text{CO}$  is the leading sink process, but this reaction does not change  $\text{HO}_x$ , and  $\text{OH}$  is well buffered w.r.t. changes in  $\text{CO}$ . For  $\text{HO}_x$ , the dominant sink processes are self-reactions of  $\text{HO}_x$  ( $\text{HO}_2 + \text{HO}_2 \rightarrow \text{H}_2\text{O}_2$ ,  $\text{HO}_2 + \text{OH} \rightarrow \text{H}_2\text{O}$ ) competing with  $\text{OH} + \text{CH}_4$ . However, the methane impact is complicated by the oxidation products. In short: a satisfying answer to this question would require a much more comprehensive investigation.

Regarding the high values of  $\text{OH}$  in figure 3, again this is for the 6 km level (where  $\text{OH}$  concentrations are larger than at the surface). We have made this explicit in the figure caption.

12. *If the  $\text{CH}_4$  observations are different from the reference simulation by only  $\sim 2\%$  please explain the reported 40% sensitivity of  $\text{OH}$  to the change in  $\text{CH}_4$ . The discussion refers to the percentage changes in  $\text{OH}$  shown in Figure 6e/6f, but these do not show percentage changes. The discussion should be consistent with the figures in terms of the way the differences are expressed. Please provide some discussion of the use of  $d \ln(\text{OH})/d \ln(\text{CH}_4)$  (or  $\text{CO}$ ) in Figure 6.*

The number of 0.4 was an error.  $\text{OH}$  increases by  $> 0.6\%$  when  $\text{CH}_4$  is increased by 2% in March (figure 6c). The relative sensitivity  $A_{\text{CH}_4} = \partial \ln \text{OH} / \partial \ln \text{CH}_4$  is no longer expressed in percent. It maximizes, in absolute terms, at  $-0.32$  (meaning the relative response of  $\text{OH}$  is up to 0.32 times the relative difference in  $\text{CH}_4$ , but opposite in direction). Regarding the use of the infinitesimal notation, this is just a straightforward reformulation of equation 2. This is now made explicit in the text.

[Printer-friendly version](#)[Discussion paper](#)

13. *Line 275: Is  $\text{OH} + \text{CH}_4$  the dominant OH sink in the model? What is the change in the kinetics of the reaction for the temperature change applied to the model?*

The reaction coefficient for  $\text{OH} + \text{CH}_4$  in the model is  $1.85 \cdot 10^{-12} \exp(-1690/T)$ . This makes it one of the most temperature-sensitive reactions in the NIWA-UKCA chemistry scheme. The sensitivity of the reaction coefficient, at 290 K, evaluates to approximately 2%/K of temperature difference. This combined with the important role of  $\text{CH}_4 + \text{OH}$  as a  $\text{HO}_x$  sink, means that indeed  $\text{CH}_4 + \text{OH}$  plays a major role in explaining the relatively small impact of temperature changes on OH. This is now made explicit in the text.

14. *Line 310: What is the significance of this equation? Can it be applied to other models? Can values for the parameters be tabulated for various altitudes (or can altitude dependent parameters be given?). How valid is the assumption that the OH response is linear to changes in the forcings? As stated, Figure 8c suggests this is not a valid assumption.*

This equation represents a working assumption; this is now made explicit in the text. We agree that there are some non-linearities, and the assumption of linearity is not perfect, but linearity explains almost the whole pattern in Figure 8 a. Other models that focus on global and background chemistry might well behave in ways similar to our model, but we haven't tested this.

15. *Line 385: Please give some examples (and references!) of underestimated  $\text{CH}_4$  lifetimes by NIWA-UKCA and comparisons with other accepted estimates. An expanded introduction will help with this.*

In the REF-C1 simulation of NIWA-UKCA used here, the  $\text{CH}_4$  lifetime evaluates to 7.6 years. This compares to 9.2 years as the best estimate from SPARC (2013). We have added text (in section 3.5) quantifying the  $\text{CH}_4$  lifetime in NIWA-UKCA and giving this best estimate. Further citations are added in the conclusions section.

[Printer-friendly version](#)[Discussion paper](#)

16. *Minor comments: Line 11: 'Its impact. . .', please change this to 'The impact of  $O_3$  . . .'* for clarity.

Done

17. *Line 32: 'in-situ' to 'in situ'.*

Done, also elsewhere.

18. *Line 60: Please spell out NIWA in full.*

Done

19. *Line 71/line 135: What determines the concentrations of these species in the model if there are no emissions? Are they constrained to observations? Set to zero?*

NIWA-UKCA model data are used for these species. This is now made explicit in the text (also in section 2.3).

20. *Page 101: 'Vertically integrated ozone produced here' – please reword, do you mean 'produced in this way'?*

We have changed 'vertically integrated ozone produced here' for 'the vertical integration of the observed O3 profiles'.

21. *Line 161: Please replace 'a' and 'b' with 'k' in keeping with convention, and label the different 'k' appropriately to distinguish between reactions (i.e.  $k_a$ ,  $k_b$  or  $k_1$ ,  $k_2$ ).*

Done

22. *Line 290: Space in '5K'.*

Done

Printer-friendly version

Discussion paper



23. *Line 329: 'sky' to 'skies'.*

Done

24. *Line 336: Please change the word 'combinedly'.*

We replace this with 'in combination'.

25. *Line 373: Please change 'chemical equilibrium' to 'chemical steady state'.*

Done

26. *Figure 1: Panel e, please remove the degree symbol.*

Done

27. *Figure 2: Panel f, presumably this should refer to panels 2b and 2d?*

Done

28. *Figure 3: Please remove the titles to the plots and leave just the labels a, b and c. See comments above regarding the exponential relationships - please give the parameters (and fit statistics) for the relationships described if these are important. If they are, why mention them?*

Done. We now state the fitting parameters, but we don't regard the fit statistics as necessary in this context as these coefficients are not used any further in the following text.

29. *Figure 4: The data shown in the plots are given as percentages in the discussion. Please see comments above regarding consistency.*

Changes of species are generally now given as percentages relative to the reference, but sensitivity coefficients are given as fractions. We think this is now handled consistently.

Printer-friendly version

Discussion paper



30. *Figure 5: Please clarify in the caption that panels e and f refer to plots a & b and c & d, respectively. The analysis  $d \ln(OH)/d \ln(H_2O)$  is not explicitly referred to in the text (likewise for Figure 6).*

We have clarified the caption and have removed the formula.

31. *Figure 6: Figure 6e in the caption is referred to as Figure 6d.*

Changed. We have reformulated the caption along the same lines as figure 5.

32. *Figure 8: Panel c, please explain the significance of the dashed and red lines.*

The significance of the red solid and black dashed lines has been explained in the caption of Figure 8.

---

Interactive comment on Atmos. Chem. Phys. Discuss., doi:10.5194/acp-2016-448, 2016.

Printer-friendly version

Discussion paper



# ***Interactive comment on “Assessing the sensitivity of the hydroxyl radical to model biases in composition and temperature using a single-column photochemical model for Lauder, New Zealand” by L. López-Comí et al.***

**L. López-Comí et al.**

olaf.morgenstern@niwa.co.nz

Received and published: 3 October 2016

*General Comments: This paper shows the influence of biases in modeled  $O_3$ ,  $H_2O$ ,  $CO$ ,  $CH_4$ , and temperature on modeled  $OH$  as investigated using a single-column model and observations over Lauder, New Zealand. Model fields of the parameters listed above are replaced with observations, and the photochemical single-column model is used to re-calculate  $OH$  and establish changes and sensitivities in  $OH$  relative to a reference run. Impacts of  $O_3$  and temperature biases are further examined by separating kinetic and photolytic effects. Long-term  $OH$  trends and effects of clouds on  $OH$  are*

Printer-friendly version

Discussion paper



*briefly examined.*

*While this analysis is somewhat limited in scope and some aspects of the discussion are quite cursory, tropospheric OH is an important issue requiring varied and novel approaches to build on the community's understanding. With some revisions, this paper would contribute a useful method to help identify how model representation of OH can be improved and why model versus empirical estimates of the CH<sub>4</sub> lifetime differ.*

We agree with the reviewer that novel approaches to understanding the diversity of OH in global models are needed; we think the approach presented here is such a novel approach. We also accept that the scope is limited, namely we only assessed OH at the Lauder observatory. Within the context of this paper this is not easily addressed. However, in a follow-up study, the approach could be rolled put to other locations albeit with caution due to issues with data availability, a necessary reliance on satellite remote sensing data, or the role of other pollutants not present above Lauder. This is dwelt on a little more in the final section of the text now. We hope the revised paper now addresses the reviewer's concern.

*Major comments:*

- 1. Line 10: Please provide some quantification for these results. Particularly useful would be an indication of how much H<sub>2</sub>O differed between the model and observations as well as a quantification of how OH changed in response. The same could be done for subsequent species.*

A quantification of biases in the key forcings and also of the OH sensitivity have been included in the abstract.

- 2. Line 47: You state two paragraphs above that "in-situ measurements of OH do not sufficiently constrain its global abundance." Here, you cite two Emerson papers that do exactly that as justification for your SCM approach. I understand that constraining OH globally is not your aim, but the two statements still seem*

*contradictory. It would be worthwhile to strengthen your justification for this analysis - what questions are you seeking to answer? What role can this approach play in constraining global OH, even if there are limitations?*

The Emmerson et al. papers are about using a box model to understand measurements of OH and HO<sub>2</sub> taken in polluted environments. It would be incorrect to assert that these papers aim to quantify global OH. Our approach is unique in that we focus on the remote atmosphere and use long-term observations to constrain the model – other approaches such as Emmerson et al. have used campaign data. We have modified the text to this effect.

3. *Line 75: The number of species and reactions represented in the NIWA-UKCA chemical mechanism seems low, at least compared to explicit schemes like the MCM (easily into the hundreds of species and thousands of reactions). Might be worth noting why it's important to maintain consistency with the NIWA-UKCA model/why you wouldn't want a more detailed mechanism in your SCM, since "assessing fast photochemistry" is your goal.*

The purpose of this work is to assess the contribution of NIWA-UKCA biases to OH. If we used a different chemical mechanism to the one used in the NIWA-UKCA model, we would be introducing more uncertainties in the analysis. Also this might make the analysis less relevant to chemistry-climate modelling in general. A sentence reporting on this has been included in the text. See paragraph 1 of section 2.1.

4. *Line 326: This section should be expanded. Even though the trends are not significant, they can still be quantified, and numbers here compared to values in the other studies you cite. Also, trends shown, for example, in Montzka et al., 2011 are derived from a globally, vertically integrated [OH] calculation, so separation into altitude bins, while useful, may not be the best comparison. I realize you don't seek to look at global [OH], but at least for this location, you could*

[Printer-friendly version](#)[Discussion paper](#)

*include a vertically integrated OH trend to compare to Montzka et al. In addition to quantifying the trend, you could also quantify the interannual variability.*

We now state numerical values for the trends. We find no significant trend in the total column, which is in general agreement with a study on global OH by Montzka et al., however noting that we do not assess global OH. We now state the magnitude of interannual variability.

5. *Line 430: The reader is likely interested to hear your hypotheses on why NIWA-UKCA is too moist and  $O_3$  is too high, even if further investigation is beyond the scope of this paper.*

We appreciate that these are interesting though difficult questions. Difficulties with the hydrological cycle can be due to surface-atmosphere or cloud-atmosphere interactions at Lauder. The ozone biases could be partly caused by the water vapour biases. We have added two sentences to this effect.

*Minor comments:*

6. *Line 11: Reference to  $O_3$ 's kinetics and photolysis effects is unclear until defined in the body of the paper; please rephrase for abstract. Assertion that both are of similar magnitude does not seem well-supported, as pointed out above.*

We have rephrased this in the abstract and now give numbers (in response to your earlier comment). These numbers do support the assertion that “both are of similar magnitude”.

7. *Line 12: Sentence about OH being inversely related to CO and  $CH_4$  is unnecessary for an audience familiar with OH.*

We have removed this sentence.

8. *Line 19: Use of “less-than-additive” is vague, especially for an abstract. Instead of focusing on how the LWC and IC effects combine, it would probably be more*

Printer-friendly version

Discussion paper



*informative to note the quantitative results of the combined LIC simulation, if that is the more realistic one. This would likely be of greater interest to the reader.*

We have removed this sentence and now quantify the impact of clouds.

9. *Line 20: Please quantify trends as well, even if they are insignificant.*

Done

10. *Line 101: use of word “produced” is unclear.*

The phrase has been replaced by “total column ozone calculated by integrating the observed O<sub>3</sub> profiles”.

11. *Line 115: You make the case for not trusting radiosonde H<sub>2</sub>O data above 8 km, but how about the NIWA-UKCA output? Does modeled H<sub>2</sub>O agree well with FPH? A figure addressing this point might be suited for supplemental material.*

NIWA-UKCA H<sub>2</sub>O is subject to biases also above 8 km. We simply do not have any observational data above this level that is of high enough quality and frequency and covers the study period. We therefore do not discuss impacts on OH above 8 km here. This is now made explicit in the text.

12. *Line 131: It would be helpful to address some anomalous behaviour in the H<sub>2</sub>O profiles shown in Fig. 1: in the winter (presumably) of 1996, and to a lesser extent in other years, there are sudden high temperatures around 40-60 km – what’s the cause of this? Is there evidence of this truly happening in the atmosphere or is it a result of interpolation, instrument artifact, etc?*

These warming events may be the result of planetary wave breaking in the upper stratosphere. The event in 1996 is covered by many satellite measurements and therefore is likely real. We have not studied these events as they are outside the scope of this paper. We have added a sentence to the text to this effect.

Printer-friendly version

Discussion paper



13. *Line 137: What are the native temporal and spatial resolutions of this simulation? Do you also interpolate spatially?*

We use 10-daily instantaneous output fields by NIWA-UKCA to construct the interpolates. The native resolution of NIWA-UKCA is  $3.75^\circ \times 2.5^\circ$ . We do not interpolate spatially. We consider the closest grid point to Lauder position. We have modified the text (section 2.1) to this effect.

14. *Line 174: Make clear that you're discussing local  $O_3$ , or the "kinetics" effect.*

We have modified the text to this effect.

15. *Line 177: The sentence "The largest impact is in the free troposphere where these differences vary with altitude." is a bit vague. Please be specific; what are the differences you're referring to, and how do they vary?*

We have removed this sentence and added more detail to this discussion.

16. *Line 188: I'm not sure what you mean by the statement that kinetics and photolysis effects of the  $O_3$  bias are comparable. Based on my interpretation of the contours in Fig. 2, the response of OH to kinetic effects is both positive and negative, depending on the month and ranges from  $-12$  to  $+4\%$ ; the response to photolysis effects is only positive, about  $4 - -16\%$ . The two effects somewhat cancel around Feb-June - is this what you're referring to? Please clarify.*

We have qualified this statement. The magnitudes of the two effects are similar but seasonalities and height dependencies differ.

17. *Line 241: The statistic that sensitivity of OH to  $CH_4$  changes peaks at  $\sim 40\%$  can be easily misinterpreted as the OH response; it may be helpful to highlight both the max OH response as well as the OH sensitivity to avoid confusion.*

We now consistently express relative changes of OH,  $O_3$  etc. as percentages, and sensitivities such as this as fractions. We have added in the text that the maximum OH difference due to correcting  $CH_4$  is  $0.6\%$ .

Printer-friendly version

Discussion paper



18. *Line 295: You stated above that the O'Connor et al. result may be due to cancellation of positive and negative temperature biases, but you show that temperatures at Lauder are cold-biased, so saying that your result of small impact of temp on OH corroborates that of O'Connor et al. seems like an apples-to-oranges comparison. I'd suggest reframing the discussion of O'Connor et al. – the small impact on OH in O'Connor et al. could have been due either to cancellation of temp biases or to low sensitivity of OH to temp changes, and your result suggests the latter? Or something to that effect.*

We have followed the reviewer's suggestion.

19. *Line 320: Care to hypothesize about what might be causing these non-linearities?*

Quite likely there are some feedbacks between correcting the water vapour and ozone biases which we now allude to in the text.

20. *Line 366: what do you mean by "slow chemistry"? My best guess is something like oxidation of CH<sub>4</sub> (long-lived), yet that is considered here, so I'm not sure about your intended meaning.*

We supply independent initial states at every iteration of the SCM, meaning that species with a local chemical lifetime longer than the timestep of 1 hour can be considered prescribed for this purpose. Hence the model is only really suitable for fast radical chemistry. We have modified the text to this effect.

21. *Line 382: Again, would like to see quantification here; how much is the H<sub>2</sub>O overestimated?*

We now give this information in the text.

22. *Line 387: Please include some references, particularly when citing "accepted literature estimates".*

Printer-friendly version

Discussion paper



Done

23. *Line 400: "...small reduction...due to the strong dependence of OH + CH<sub>4</sub> on temperature." This does not logically follow; you'd think, with a strong dependence, that you should see a large reduction. Please clarify.*

It's been rephrased in paragraph 6 of the conclusions.

24. *Line 406: Thank you for quantifying the H<sub>2</sub>O bias! I think this statistic would be better suited to earlier paragraph on H<sub>2</sub>O, plus repeat in Section 3 and in abstract.*

We have now added this information in the abstract and in section 3.

25. *Fig. 2: The use of both blue and red for strictly positive values is slightly confounding at first glance (panels (c)-(f)); if possible, would help to keep the white contour at value 0 (applies to various upcoming figures as well).*

We have changed all such plots displaying the OH sensitivity to changes in the forcings, i.e. keeping the white contour at value 0, and blue and red colour levels for negative and positive values respectively.

26. *Table 1: Is the O<sub>3</sub> photolysis effect analysis done in an altitude-dependent manner? I.e., is a new  $j_{O1D}$  value calculated at each vertical point based on an overhead O<sub>3</sub> column that's adjusted to account for the strat column plus the partial tropospheric column overhead? I did not see any details regarding this in the text.*

The  $j_{O1D}$  values are calculated at each altitude level, so it is taking into account the stratospheric contribution and the corresponding partial tropospheric column for each level. A sentence stating this has been added in the text. See section 2.1.

27. *Fig. 5: Use of  $d \ln(OH)/d \ln(H_2O)$  is not mentioned in text, is not consistent with "A<sub>i</sub>" terms in Fig. 4; please either justify switching metrics or maintain consistency*

Printer-friendly version

Discussion paper



(same with Fig. 6).

We have added eq. 3, which basically states an alternative, equivalent way of formulating  $A_i$ .

Also we now consistently use percentages to indicate model biases (except for temperature) and fractions to indicate model sensitivities  $A_i$ .

28. *Fig. 9: y-axis label is misleading since, based on the caption, this shows OH anomalies. Perhaps include word “Anomaly” or a “delta” sign. Also, the values chosen for the y-axis tick marks are not easy to work with; it would be nice if they were adjusted to lie along round calculation-friendly values (e.g. increments of 0.5 instead of 0.417 in panel c). Also, how are these anomalies calculated, relative to what?*

We have relabelled plot 9c. These are absolute differences in units of  $10^5$  molecules/cm<sup>3</sup>.

*Technical corrections:*

29. *Line 23: Use of word atmospher-e/-ic 3x*

We have rephrased the sentence.

30. *Line 29: “plays a important” should be “plays an important”*

Done

31. *Line 50: “long time series” wording seems off; perhaps “long record of observation” instead. I’m also curious at this point, how long is long? Perhaps give an earliest year of observation.*

This has been changed to “long records of measurements are available since 1986”. We use data since 1994 in this work as MOPI1 measurements started in 1994.

Printer-friendly version

Discussion paper



32. *Line 53: I think “Section 1” should be “Section 2”?*  
Corrected.
33. *Line 250: “altitide” should be “altitude”*  
Done
34. *Line 256: spelling of the word “assess” is incorrect*  
Done
35. *Line 275: use of “explicitly” does not add meaning to this sentence but makes it read awkwardly; I suggest removing.*  
Done
36. *Line 279: “nearly completely linearly” should be “nearly linearly”*  
Done
37. *Line 324: instead of “altitude bands”, I more often see the phrase “altitude bins”*  
Done
38. *Line 378: use of word “effect” doesn’t seem quite right; it’s the bias you’re correcting.*  
Done

---

Interactive comment on Atmos. Chem. Phys. Discuss., doi:10.5194/acp-2016-448, 2016.

Printer-friendly version

Discussion paper



# Assessing the sensitivity of the hydroxyl radical to model biases in composition and temperature using a single-column photochemical model for Lauder, New Zealand

L. López-Comí<sup>1,2</sup>, O. Morgenstern<sup>1,\*</sup>, G. Zeng<sup>1,\*</sup>, S. L. Masters<sup>2</sup>, R. R. Querel<sup>1</sup>, and G. E. Nedoluha<sup>3</sup>

<sup>1</sup>National Institute of Water and Atmospheric Research (NIWA), Lauder, New Zealand

<sup>2</sup>Department of Chemistry, University of Canterbury, Christchurch, New Zealand

<sup>3</sup>United States Naval Research Laboratory, Washington, DC, United States

\* now at NIWA, Wellington, New Zealand

*Correspondence to:* O. Morgenstern (olaf.morgenstern@niwa.co.nz)

**Abstract.** We assess the major factors contributing to local biases in the hydroxyl radical (OH) as simulated by a global chemistry-climate model, using a single-column photochemical model (SCM) analysis. The SCM has been constructed to represent atmospheric chemistry at Lauder, New Zealand, which is representative of the background atmosphere of the Southern Hemisphere (SH) mid-latitudes. We use long-term observations of variables essential to tropospheric OH chemistry, i.e. ozone (O<sub>3</sub>), water vapour (H<sub>2</sub>O), methane (CH<sub>4</sub>), carbon monoxide (CO), and temperature, and assess how using these measurements affect OH calculated in the SCM, relative to a reference simulation only using modelled fields. The analysis spans 1994 to 2010. Results show that OH responds approximately linearly to correcting biases in O<sub>3</sub>, H<sub>2</sub>O, CO, CH<sub>4</sub>, and temperature. The biggest impact on OH is due to correcting **an overestimation by approximately 20 to 60% of H<sub>2</sub>O**, using radiosonde observations. **Correcting this moist bias leads to a reduction of OH by around 5 to 35%.** This is followed by correcting **predominantly overestimated O<sub>3</sub>. In the troposphere, the model biases are mostly in the range of -10 to 30%.** ~~Its~~**The impact of changing O<sub>3</sub> on OH is due to two pathways; the OH responses to both are of similar magnitude but different seasonality: Correcting in situ tropospheric ozone leads changes in OH in the range -14 to 4%, whereas correcting the photolysis rate of O<sub>3</sub> in accordance with overhead column ozone changes leads to increases of OH of 8 – 16%.** The OH sensitivity to correcting CH<sub>4</sub> and CO biases is inversely related to the relative changes applied to these species; **are both minor effects.** The work demonstrates the feasibility of quantitatively assessing OH sensitivity to biases in longer-lived species, which can help to explain differences in simulated OH between global chemistry models and relative to observations. In addition to clear-sky simulations, we have performed idealised sensitivity simulations to assess the impact of clouds (ice and liquid) on OH. The results indicate that the impacts on the ozone photolysis rate and OH are substantial, with a general decrease of OH below

the clouds **of up to 30%** relative to the clear-skies situation, and an increase **of up to 15%** above.

25 ~~The effects of liquid and ice clouds are less than additive.~~ Using the SCM simulation we calculate recent OH trends at Lauder. For the period of 1994 to 2010, all trends are insignificant, in agreement with previous studies. **For example, the trend in total-column OH is  $0.5 \pm 1.3\%$  over this period.**

## 1 Introduction

The hydroxyl radical (OH) is essential to atmospheric chemistry as the leading atmospheric oxidantizing  
30 ~~in the atmosphere agent.~~ It acts as a “detergent”, reacting with numerous, mostly organic pollutants (Levy, 1971; Logan et al., 1981; Thompson, 1992; Lelieveld et al., 2004; Naik et al., 2013) and controls the lifetimes of many trace gases containing carbon-hydrogen bonds, because reaction with OH is their dominant removal mechanism. It is also responsible for oxidizing atmospheric trace gases such as carbon monoxide (CO), non-methane volatile organic compounds (NMVOCs), and also some ozone-depleting substances such as hydrochlorofluorocarbons (HCFCs) (DeMore, 1996). Therefore, the oxidizing capacity of the atmosphere is largely  
35 ~~determined~~ defined by the abundance of OH radicals. Tropospheric ozone ( $O_3$ ), an air pollutant and greenhouse gas (GHG), is the primary source of OH in the troposphere. **Although it only accounts for 10% of the total atmospheric  $O_3$  abundance, it plays an essential role in photochemical processes controlling tropospheric composition.** It forms OH via  $O_3$  photolysis yielding excited oxygen ( $O(^1D)$ ) and a subsequent reaction of  $O(^1D)$  with water vapour ( $H_2O$ ).  **$CH_4$  and CO oxidation by OH, and other oxidation processes involving NMVOCs, lead to formation of tropospheric  $O_3$  in the presence of  $NO_x$  (Logan et al., 1981; Thompson, 1992; Lelieveld and Dentener, 2000). In low- $NO_x$  atmospheric environments, such as in much of the Southern  
45 Hemisphere, downward transport of  $O_3$  from the stratosphere is the main source of tropospheric  $O_3$ , followed by  $O_3$  transport from other regions where it is chemically produced (Zeng et al., 2010). Stratospheric  $O_3$  also plays an important role through its impact on the  $O_3$  photolysis rate  $j_{O^1D}$  which is affected by the overhead  $O_3$  column. **For instance, stratospheric  $O_3$  depletion produces increased UV penetration to the troposphere. This affects the production of tropospheric OH.****

The most widely used technique for field measurements of OH is called the Fluorescence Assay by Gas Expansion (FAGE) and is based on the measurement of OH and other species concentrations through laser induced fluorescence spectroscopy. OH measurements using the FAGE technique have been conducted in a large variety of atmospheric environments, ranging  
55 from polluted (Ren et al., 2003; Dusanter et al., 2009) to clean (Creasey et al., 2003; Bloss et al., 2007) atmospheres. However, due to its very short lifetime (the global lifetime is estimated to be  $\sim 1$  s, Prinn, 2001; Elshorbany et al., 2012) and large variability, such in situ measurements of OH do not sufficiently ~~constrain~~ capture its global abundance, which makes it difficult to

sufficiently constrain global OH abundances with in situ measurements (Heard and Pilling, 60 2003). For that reason, modelling is an essential tool to study global OH. OH is routinely included in global models of tropospheric chemistry, but the complexity of the tropospheric chemical system and the sensitivity of OH to a variety of environmental factors mean that there is considerable disagreement among global chemistry-transport and chemistry-climate models regarding the global OH abundance; this is often expressed in terms of the CH<sub>4</sub> lifetime (e.g., Stevenson et al., 65 2006; Naik et al., 2013; Voulgarakis et al., 2013). Several model studies have examined changes in OH abundance and the CH<sub>4</sub> lifetime since pre-industrial times. Chemistry-transport models (which use off-line, precalculated meteorology) generally simulate decreases in OH and increases in the CH<sub>4</sub> lifetime, ranging from 6% to 25% during the 21<sup>st</sup> century (Thompson, 1992; Lelieveld et al., 1998; Wild and Palmer, 2008). These results differ from those produced 70 by chemistry-climate models which account for changes in both emissions and climate (Stevenson et al., 2000; Johnson et al., 2001; Shindell et al., 2006; Zeng et al., 2010; John et al., 2012). All of them project a reduction in the CH<sub>4</sub> lifetime and an increase in OH. In particular, Shindell et al. (2006) and Zeng et al. (2010) obtain a ~10% decrease in the CH<sub>4</sub> lifetime using different emission scenarios in their simulations. More recent and comprehensive studies compare present-day and future results for OH and the CH<sub>4</sub> lifetime among models participating 75 in the Atmospheric Chemistry and Climate Model Intercomparison Project (ACCMIP, Naik et al., 2013; Voulgarakis et al., 2013). Naik et al. (2013) analyse the evolution of the CH<sub>4</sub> lifetime and OH in ACCMIP models since preindustrial times (1850-2000). They point out large variations in the sign and magnitude of OH changes (from -12.7% to 14.6%) amongst AC- 80 CMIP models, reflecting uncertainties in natural CO, NO<sub>x</sub>, and NMVOC emissions as well as roles of the diverse chemical mechanisms included in the models. For present-day (year 2000) simulations of OH and the CH<sub>4</sub> lifetime, Voulgarakis et al. (2013) suggest that diversity in photolysis schemes and NMVOC emissions might cause large variations in simulated OH and the CH<sub>4</sub> lifetime. Trends in OH between 2000 and 2100 are mainly attributed to stratospheric 85 O<sub>3</sub> changes and trends in modelled temperature fields.

A useful indirect method for determining constraining global OH is based on tracking the abundance of long-lived, well-mixed chemicals for which oxidation by OH is the dominant sink and which have a well-quantified, industrial source. The most widely used such species is methyl chloroform (CH<sub>3</sub>CCl<sub>3</sub>) (Prinn et al., 2005; Bousquet et al., 2005; Manning et al., 2005; Krol et al., 90 2008). Montzka et al. (2011) use CH<sub>3</sub>CCl<sub>3</sub> measurements to infer only a small interannual variability in OH for 1998-2007. The global multi-model mean OH inferred from the ACCMIP ensemble (Naik et al., 2013) increases slightly ( $3.5 \pm 2.2\%$ ) over the period 1980-2000. This result largely agrees with Montzka et al. (2011) and with other models (Dentener et al., 2003; Hess and Mahowald, 2009; John et al., 2012; Holmes et al., 2013), but disagree with other studies of 95 CH<sub>3</sub>CCl<sub>3</sub> observations that find a decrease in OH over that period (Prinn, 2001; Bousquet

et al., 2005). For the year 2000, Naik et al. (2013) underestimate the  $\text{CH}_3\text{CCl}_3$  lifetime (and thus overestimate OH) by 5% to 10% relative to observations.  $\text{CH}_3\text{CCl}_3$  is controlled under the Montreal Protocol, meaning its abundance in the atmosphere is approaching the detection limit and it will no longer be a useful constraint on OH in decades to come.

100 A further indirect method to address OH is to measure  $^{14}\text{CO}$ . Manning et al. (2005) find some considerable variability but no long-term trend using this method. According to Krol et al. (2008), this method is considerably more sensitive to high-latitude than low-latitude OH, in contrast to the  $\text{CH}_3\text{CCl}_3$  method which is mostly sensitive to tropical OH.

Addressing **Therefore, a step forward in addressing** the uncertainty in modelling OH in global  
105 **models is to quantitatively assess the contributions of biases in long-lived species that are central to OH. This** sometimes involves juxtaposing them **global models** to local-scale (box or single-column) models constrained **as much as possible** by observations and incorporating only fast photochemical processes. **For example**, Emmerson et al. (2005, 2007) **develop a box model to assess the sensitivity of OH and  $\text{HO}_2$  to biases in long-lived species, and compare the model results**  
110 **to observations. However, their analyses only pertain to polluted environments not representative of much of the global atmosphere and only take in episodic and surface measurements. Single-column models have been applied to modelling the atmospheric boundary layer (Mihailovic et al., 2005; Cuxart et al., 2006), diabatic processes (Randall et al., 2003; Bergman and Sardeshmukh, 2004), clouds and aerosols (Kylling et al., 2005; Lebassi-Habtezion and**  
115 **Caldwell, 2015; Dal Gesso et al., 2015), the impacts of GHGs on climate change (Vupputuri et al., 1995), and the chemistry of halogen compounds (Piot and von Glasow, 2008; Joyce et al., 2014). Tropospheric OH chemistry of the remote atmosphere has not been assessed in a single-column model framework before.**

In the present paper, we introduce and evaluate a single-column model (SCM) constrained with  
120 available long-term observations at Lauder, New Zealand ( $45^\circ\text{S}$ ,  $170^\circ\text{E}$ , 370 m above sea level), **to investigate how chemistry-climate model biases in long-lived chemical species and temperature affect OH.** Lauder is known for its clean air (Stedman and McEwan, 1983; McKenzie et al., 2008), and large diversity of available measurements (it is part of the Network for the Detection of Atmospheric Composition Change (NDACC), Badosa et al., 2007; McKenzie et al.,  
125 **2008; Organization, 2011).** Observations made at Lauder include UV radiation and surface, **profile, and/or total columns of  $\text{O}_3$  and several other species.** and, ~~f~~The  $\text{O}_3$ ,  $\text{H}_2\text{O}$ , and **temperature records produced by ozone sondes cover 1986 to the present. Lauder therefore** is ideal for this kind of study. The SCM is built around a medium-complexity stratosphere-troposphere chemistry scheme. The model is forced with Lauder observations and/or output from a chemistry-climate  
130 model that uses the same scheme (see below). In Section 2, we describe the set-up of the SCM, the construction of time series of key species and meteorological parameters that drive the SCM, and

the simulations. In Section 3, we present results of simulated OH concentrations and trends from the SCM and analyse the sensitivity of OH to various forcings. Conclusions are gathered in Section 4.

## 2 Models and simulations

### 135 2.1 The single-column photochemical model (SCM)

The single-column photochemical model (SCM) is a stand-alone version of the stratosphere-troposphere chemistry mechanism used by the **National Institute of Water and Atmospheric Research - United Kingdom Chemistry and Aerosol (NIWA-UKCA)** model, which comprises gas-phase photochemical reactions relevant to the troposphere and stratosphere (Morgenstern et al., 2009, 2013; 140 Telford et al., 2013; O'Connor et al., 2014; Morgenstern et al., 2016). **For consistency with NIWA-UKCA, the SCM uses the same chemical mechanism. Had we used a more complex mechanism (which the SCM approach lends itself to), then a direct comparison with the NIWA-UKCA output would no longer be possible, and also the results would be less relevant to other global CCMs characterized by relatively simple chemical mechanisms.** The 60 vertical levels 145 of the SCM are the same as in NIWA-UKCA, extending to 84 km. **We do not use horizontal interpolation and take profiles of atmospheric properties from the gridpoint closest to Lauder (45°S,168.75°E).** Unlike NIWA-UKCA, the SCM excludes all non-chemistry processes, such as transport, dynamics, the boundary-layer scheme, radiation, emissions, etc. This means the model is only suitable for assessing fast photochemistry. **Forcing data for the SCM are mostly interpolated 150 from 10-daily instantaneous outputs from a NIWA-UKCA simulation (see below), except for those fields for which observational data are used.**

Morgenstern et al. (2013) and O'Connor et al. (2014) describe the chemistry scheme included in the SCM. The SCM includes an isoprene oxidation scheme (Pöschl et al., 2000; Zeng et al., 2008; Morgenstern et al., 2016) not included in the NIWA-UKCA model version used by Morgenstern 155 et al. (2013). In addition to CH<sub>4</sub> and CO, the model includes a number of primary non-methane volatile organic compound (NMVOC) source gases, i.e. ethane (C<sub>2</sub>H<sub>6</sub>), propane (C<sub>3</sub>H<sub>8</sub>), acetone (CH<sub>3</sub>COCH<sub>3</sub>), formaldehyde (HCHO), acetaldehyde (CH<sub>3</sub>CHO), and isoprene (C<sub>5</sub>H<sub>8</sub>). As noted above, emission and deposition of species are not considered in the SCM. The SCM includes a comprehensive formulation of stratospheric chemistry (Morgenstern et al., 2009) comprising bromine 160 and chlorine chemistry and heterogeneous processes on liquid sulfate aerosols. Overall, the model represents 86 chemical species and 291 reactions including 59 photolysis and 5 heterogeneous reactions. The FAST-JX interactive photolysis scheme (Neu et al., 2007; Telford et al., 2013) has been implemented in the SCM; **this scheme solves a radiative transfer equation accounting for absorption by ozone.** The chemical integration is organised through a self-contained atmospheric chemistry package (Carver et al., 1997), and the differential equations describing chemical kinetics 165 are solved using a Newton-Raphson solver (Morgenstern et al., 2009).

## 2.2 Construction of vertical profiles of forcing species and meteorological parameters

Time series of  $O_3$ ,  $H_2O$ ,  $CO$ , and temperature profiles are produced using mainly long-term measurements from Lauder, supplemented with NIWA-UKCA results as detailed below. Lauder is a member of several international networks, including the Network for the Detection of Atmospheric Composition Change (NDACC; <http://www.ndsc.ncep.noaa.gov>), the Global Reference Upper Air Network (GRUAN; <http://www.gruan.org>), and Global Atmosphere Watch (GAW; [http://www.wmo.int/pages/prog/arep/gaw/gaw\\_home\\_en.html](http://www.wmo.int/pages/prog/arep/gaw/gaw_home_en.html)), where these data are archived and made available. The networks coordinate long-term observations of  $O_3$ , various other constituents, and meteorological parameters. Here we briefly describe the procedure of constructing forcing data, using Lauder observations, to be used to constrain the SCM. The resulting profiles are shown in Fig. 1.

$O_3$  profiles used here are a combination of ozonesonde time series (from the surface to 25 km, Bodeker et al., 1998) combined with the Microwave Ozone Profiler Instrument 1 (MOPI1) time series for altitudes above 25 km (Boyd et al., 2007; Nedoluha et al., 2015), covering 1994 to 2010 (Fig. S1a). The ozone sondes have been launched approximately weekly; this defines the temporal coverage of the forcing data used in the SCM calculations. Microwave measurements used here come as several profiles a day at a variable spacing; we interpolate them to the ozone sonde launch times. Any missing data (during the two periods when the microwave instrument was out of service) are filled using a Fourier series gap-filling method. We compare the two datasets in the height region usefully covered by both (20 to 30 km). The differences between the two measurements range between  $-2\%$  and  $+6\%$ , and a mean bias that is less than  $5\%$ .  $O_3$  profiles are linearly interpolated onto the SCM's grid. **Total column ozone calculated by integrating the observed  $O_3$  profiles** Vertically integrated ozone produced here is also compared to total-column  $O_3$  ozone measured by the Lauder Dobson instrument; the difference is about  $5\%$  on average (López Comí, 2016). Lauder ozone measurements have been used in various World Meteorological Organization (WMO) ozone assessments (e.g., Organization, 2011).

$H_2O$  profiles have been constructed using the weekly radiosonde measurements of  $H_2O$  vapour below 8 km (the same soundings that also measure ozone) and NIWA-UKCA model output data above. For validation, we use the monthly National Atmospheric and Oceanic Administration (NOAA) Frost Point Hygrometer (FPH)  $H_2O$  vapour measurements (Vömel et al., 2007; Hall et al., 2016) which start in 2003. FPHs are more accurate compared to radiosonde hygrometers, particularly for stratospheric conditions. However, due to the later start of the FPH time series and the lower measurement frequency, radiosonde measurements are used in this study. The comparison of FPH and radiosonde  $H_2O$  reveals differences that are generally less than  $\pm 5\%$  in the lower and middle troposphere but **generally** increase in and above the tropopause region ( $\sim 11$  km, López Comí, 2016). The radiosonde hygrometers have some known problems with measuring low humidity (Miloshevich et al., 2001). **This is reflected in the large differences observed particularly at these altitudes (up to 30%), and to a lesser degree, below them (Fig. 2a). In a comparison of NIWA-UKCA**

output with FPH H<sub>2</sub>O, larger discrepancies are found throughout the whole troposphere and tropopause region (Fig. 2b), as can be expected from a low-resolution model unconstrained by observations and subject to problems with modelling H<sub>2</sub>O. Given the consistency of FPH and radiosonde H<sub>2</sub>O below 8 km found above, here we use radiosonde data up to 8 km of altitude merged, in the absence of a more suitable dataset, with, and NIWA-UKCA output above that.

We use surface in situ measurements from Cape Grim, Tasmania (Cunnold and et al., 2002) to rescale NIWA-UKCA model profiles, producing CH<sub>4</sub> profiles that coincide with the ozone sonde launches. The NIWA-UKCA model simulation had been constrained with historical global-mean surface CH<sub>4</sub> values, resulting in an overestimation relative to the Cape Grim data by ~2% (not shown), and both data show a ~5% increase in CH<sub>4</sub> at the surface over the period between 1994 and 2010. Cape Grim CH<sub>4</sub> is a good surrogate for the Lauder measurements because CH<sub>4</sub> is a long-lived, well-mixed atmospheric constituent.

The time series of CO profile over the period of 1994-2010 has been constructed using the NIWA-UKCA CO profiles, rescaled such that the total columns match those obtained from the mid-infrared Fourier Transform Spectrometer (FTS) at Lauder (Rinsland et al., 1998; Zeng et al., 2012; Morgenstern et al., 2012). Gaps in the total-column FTS series, such as the period between 1994 and 1996 when the FTS measurements had not started yet, are filled using a regression fit accounting for the mean annual cycle (modelled as a 6-term harmonic series) and the linear trend.

The time series of temperature profiles are constructed following the same procedure as used in the construction of O<sub>3</sub> profiles, comprising the radiosonde temperature profiles (from the surface to 25 km) merged with NCEP/NCAR reanalyses (Kalnay et al., 1996) microwave-radiometer temperatures used in the retrieval of MOPII ozone (above 25 km) for the period of 1994-2010. From near the stratopause upwards the NCEP/NCAR temperatures are merged with a mesospheric climatology based on local LIDAR measurements. There are some warm anomalies occurring in the data at 40-60 km during winter months (e.g. in 1996); these may reflect planetary wave breaking in the upper stratosphere.

### 2.3 Simulations

We perform SCM simulations covering the period of 1994-2010, summarized in Table 1. The forcing data needed by the SCM consist of profile series of temperature, pressure, optionally cloud liquid and ice mass mixing ratios, and the mixing ratios of 86 chemical compounds. With the exceptions detailed below, these fields and species are taken from a NIWA-UKCA simulation for the period of 1994-2010 interpolated to the times of the ozone sonde launches. The CCM simulation used here consists of the last 17 years of a NIWA-UKCA "REF-C1" simulation conducted for the Chemistry-Climate Model Initiative (CCMI; Eyring and et al., 2013). REF-C1 is a hindcast simulation for the period of 1960 to 2010, using prescribed Hadley Centre sea Ice and Sea Surface Temperature (HadISST) fields (Rayner et al., 2003). The surface emissions of primary species are as described

240 in Eyring and et al. (2013), ozone-depleting substances (ODSs) follow the A1 scenario of the World Meteorological Organisation (WMO) Report (Organization, 2011), and surface (or bulk, in the case of CO<sub>2</sub>) abundances of greenhouse gases (GHGs) follow the “historical” Intergovernmental Panel on Climate Change (IPCC) scenario of global-mean GHG mixing ratios (Meinshausen et al., 2011).

In a “reference” simulation of the SCM all forcings are taken from this REF-C1 simulation of 245 NIWA-UKCA. Alternatively, in sensitivity simulations O<sub>3</sub>, H<sub>2</sub>O, CH<sub>4</sub>, CO, and temperature, or all of these simultaneously, are replaced with the time series of the profiles that are constructed using long-term observational data as described above. For species other than those 5 fields, in all cases we use NIWA-UKCA REF-C1 forcings. We evaluate the SCM only for those times, spaced roughly weekly, for which ozone sonde data are available. With the exceptions of those simulations assessing 250 cloud influences, simulations are conducted assuming clear-sky conditions.

### 3 OH sensitivity to correcting chemistry-climate model biases

In this section, we present sensitivity studies to assess the contribution of biases in known factors (O<sub>3</sub>, H<sub>2</sub>O, CH<sub>4</sub>, CO, and temperature) affecting OH photochemistry at Lauder. The response of OH to changes in each forcing is assessed individually and also in combination.

#### 255 3.1 OH sensitivity to O<sub>3</sub> biases

Three sensitivity simulations are conducted to quantify the impact of O<sub>3</sub> biases (defined as differences between observed O<sub>3</sub> and NIWA-UKCA simulated O<sub>3</sub>) on OH at Lauder.

As discussed above, the rate of production  $P$  of HO<sub>x</sub> via O(<sup>1</sup>D) + H<sub>2</sub>O can be expressed as

$$P(\text{HO}_x) \approx \frac{2k_1 j_{O^1D} [\text{O}_3] [\text{H}_2\text{O}]}{k_2 [\text{O}_2] + k_3 [\text{N}_2] + k_1 [\text{H}_2\text{O}]} \quad (1)$$

260 where  $k_1$  is the rate coefficient for O(<sup>1</sup>D) + H<sub>2</sub>O,  $j_{O^1D}$  is the rate of O<sub>3</sub> photolysis producing O(<sup>1</sup>D), and  $k_2$  and  $k_3$  are the rate coefficients of quenching of O(<sup>1</sup>D) with O<sub>2</sub> and N<sub>2</sub>, respectively (Liu and Trainer, 1988; Thompson et al., 1989; Madronich and Granier, 1992; Fuglestedt et al., 1994). Accordingly,  $P(\text{HO}_x)$  is affected by ozone changes principally in two different ways: Either locally through a change in [O<sub>3</sub>] or non-locally through a change in  $j_{O^1D}$  caused by changes in the 265 overhead total-column ozone (TCO). To separate the effects, we conduct three simulations with the SCM: The first simulation targets the local kinetics effect by applying changes in O<sub>3</sub> concentrations but keeping all photolysis rates unchanged versus the reference simulation. A second simulation involves applying changes in  $j_{O^1D}$  according to changes in O<sub>3</sub> (keeping the rest of photolysis rates unchanged), but considering a fixed O<sub>3</sub> concentration, i.e. using the O<sub>3</sub> concentrations of the refer- 270 ence simulation. **The  $j_{O^1D}$  calculation consistently takes into account absorption and scattering by stratospheric and tropospheric O<sub>3</sub>.** A third simulation includes both effects simultaneously.

The results of these three sensitivity runs are displayed in Fig. 3. As expected, the pattern of O<sub>3</sub> differences **between observed O<sub>3</sub> and modelled O<sub>3</sub>** (Fig. 3a) is reflected in the pattern of

OH differences produced by the SCM, considering only the “kinetics” effect and assuming no  
275 changes in the photolysis rates (Fig. 3b), with increases of ozone in spring and decreases in autumn,  
relative to the reference simulation, resulting in changes of the same sign in OH. However, there is  
a height dependence to this relationship. ~~The largest impact is in the free troposphere where these  
differences vary with altitude.~~ In summer and autumn,  $O_3$  biases range between  $-5\%$  and  $-45\%$ ,  
meaning that the reference simulation overestimates the observations. Such a bias in  $O_3$  results in  
280 up to 12% reductions in OH for these seasons when the bias is corrected. In spring **between 2 and  
6 km**, observed  $O_3$  is larger than in the reference simulation by up to 10% **at 4 km in October**.  
Consequently, this results in an  $\sim 5\%$  increase of OH **at around the same altitudes and times of  
up to 5%**.

Regarding the sensitivity simulation considering the photolysis effects,  $j_{O^1D}$  exhibits differences  
285 relative to the reference simulation ranging from  $\sim 14\%$  to  $\sim 30\%$ . The corrections are positive  
everywhere, in accordance with the overestimation of TCO in the NIWA-UKCA model with respect  
to observations (Morgenstern et al., 2013; Stone et al., 2016). ~~Therefore, the OH increases in Fig.  
3(d) are the result of increases in  $j_{O^1D}$ .~~ **In accordance with eq. 1, such an intensification of  $j_{O^1D}$   
causes OH to increase** (Fig. 3c). The relative OH response is approximately 50% of the  $j_{O^1D}$   
290 relative difference. However, Figs. 3(c) and (d) suggest that the magnitudes of the kinetics and the  
photolysis effects, for the  $O_3$  bias found at Lauder, are comparable, **but the seasonalities differ**.  
**For example, the kinetics effect maximizes in spring at 5% and minimizes in summer/early  
autumn at  $-15\%$  (in the upper troposphere) whereas the photolysis effect on OH maximizes  
in summer at 16 to 20% and minimizes in spring (figs. 3b and 3d).**

295 OH resulting from the combined kinetics and photolysis effects is displayed in Fig. 3(e). OH  
responds approximately linearly to the two effects combined, compared to the sum of their individual  
impacts (Fig. 3f), despite some small differences between Fig. 3(e) and (f).

Next, we examine the relationship between slant column of  $O_3$  (SCO),  $j_{O^1D}$ , and OH. Fig. 4(a)  
shows that there is an approximately exponential relationship between  $j_{O^1D}$  and the SCO at 6 km  
300 of altitude (this effect also exists at other altitudes). The small curvature may be the result of in-  
accurately diagnosing the SCO (ignoring the curvature of the Earth). Another reason could be that  
the cross section of  $O_3$  is wavelength dependent, and consequently the actinic flux spectrum moves  
towards longer wavelengths with increasing SCO. **Under Lambert-Beer’s Law, a perfectly expo-  
nential relationship would be expected for a monochromatic UV light source and an isothermal  
305 atmosphere.**  $j_{O^1D}$  and the OH concentration exhibit an approximately linear relationship (eq. 1, fig.  
4b). Combining these results, we derive an approximately exponential relationship between the SCO  
and the OH concentration (fig. 4c). **The fit parameters are stated in fig. 4. Due to the compact  
relationship between  $j_{O^1D}$  and the SCO, and to account for the curvature, we fit a quadratic  
relationship between the SCO and  $\log(j_{O^1D})$ .**

310 To determine a simple coefficient that describes the quantitative contribution of  $O_3$  to OH, a linear regression between differences in OH and  $O_3$  relative to the reference was conducted through the following expression (note that this equation is also used to derive the linear contributions of the other key species to OH chemistry at Lauder):

$$\frac{\Delta[\text{OH}]}{[\text{OH}]_{ref}} = A_i \frac{\Delta X_i}{X_{i,ref}} \quad (2)$$

315 where  $X_i$  is the perturbation variable (in this case  $[O_3]$ ),  $A_i$  is the slope of the linear regression,  $\Delta[\text{OH}]$  is the absolute difference between the OH concentrations in the reference and perturbation simulations,  $\Delta X$  is the absolute difference in concentrations of the perturbation variable  $X$  between the observations and the reference,  $[\text{OH}]_{ref}$  is the OH concentration obtained from the reference simulation, and  $X_{i,ref}$  is the value of  $X_i$  in the reference simulation. The regression coefficients  $A_i$   
 320 represent the sensitivity of OH to changes in each individual variable for the troposphere at Lauder. The regression coefficients are depicted in Fig. 5. **Reverting to infinitesimal notation, we note that**

$$A_i = \frac{\partial \ln[\text{OH}]}{\partial \ln X_i}. \quad (3)$$

325 The sensitivity coefficients of OH to the kinetics and photolysis effects of  $O_3$  are shown in Fig. 5(a). Coefficient  $A_1$ , which represent the kinetics effect, ranges from 0 to 0.25 (meaning the relative response of OH is up to a quarter of the relative difference in  $O_3$ ). The sensitivity to photolysis ( $A_1''$ ) is  $> 0.5$  throughout much of the troposphere (meaning the relative response in OH is over half the relative change in  $j_{O^1D}$ ).

### 330 3.2 OH sensitivity to $H_2O$ biases

A perturbation simulation was performed using combined radiosonde and NIWA-UKCA  $H_2O$  (section 2.2). The OH response to correcting  $H_2O$  biases (Fig. 6) shows an approximately linear response with respect to the relative changes in  $H_2O$ , i.e. decreases in  $H_2O$  generally lead to a reduction of OH concentrations (eq. 1). Note that NIWA-UKCA substantially overestimates the radiosonde-observed  
 335  $H_2O$  vapour by up to 60% between 2 and 6 km (Fig. 6a); this translates into an overestimation of OH by up to  $\sim 40\%$  in the reference simulation (Fig. 6c) in the same region. The sensitivity of OH to changes in  $H_2O$  (eq. 2) range from 5 to 0.5 in the troposphere (Figs. 6e and 5 (b) coefficient  $A_2$ ), with high sensitivity in the lower and free troposphere and reduced sensitivity in the tropopause region.

340 It is known that large uncertainties are associated with  $H_2O$  vapour measurements. To illustrate this, we repeat the above simulation but now using European Centre for Medium-Range Weather Forecasts (ECMWF) ERA-Interim reanalysis (hereafter ERAI) (Dee and et al., 2011)  $H_2O$ . Irrespectively of the large differences and the opposite signs in  $H_2O$  biases between Lauder radiosonde

and ERAI data, the OH response to biases in H<sub>2</sub>O show approximately the same linear relationship  
345 in both cases (Fig. 6). Likewise, the sensitivity of OH to changes in H<sub>2</sub>O using ERAI data (Figs. 6f)  
and 5b, coefficient  $A_3$ ) resembles the sensitivity simulation using radiosonde H<sub>2</sub>O.

### 3.3 OH sensitivity to CH<sub>4</sub> and CO biases

The effect of CH<sub>4</sub> changes on OH is displayed in Fig. 7 (a,c,e). The CH<sub>4</sub> biases are generally small,  
up to only  $\sim 2\%$ , and are assumed to be vertically uniform, with some seasonal variations. Decreases  
350 in CH<sub>4</sub> lead to increases in OH due to reduced loss of HO<sub>x</sub> by CH<sub>4</sub> + OH. The response of OH  
to CH<sub>4</sub> changes maximizes at **0.6%** around 2 km, and decreases at higher altitudes. The seasonal  
variation of the OH response to CH<sub>4</sub> biases maximizes in March/April (Fig. 7c), which coincides  
with the maximum **absolute** bias in CH<sub>4</sub> (Fig. 7a) in the same months. ~~However, the sensitivity of~~  
~~OH to CH<sub>4</sub> changes maximizes in May/June (Fig. 7e), with a peak value of  $\sim 0.4$ .~~ The sensitivity  
355 coefficient describing the dependence of OH to CH<sub>4</sub> changes (denoted as  $A_4$  in Fig. 5c) ranges from  
 $-0.17$  at the surface to  $-0.32$  at  $\sim 2$  km of altitude, and then decreases to  $-0.15$  at 10 km.

The CO bias and the resulting differences in OH are displayed in Fig. 7(b,d,f). The relative dif-  
ference of OH with respect to the reference simulation is less than  $\pm 5\%$  for all seasons (Fig. 7d),  
showing that decreases in CO generally lead to increases in OH through the reduced loss of OH  
360 through OH + CO. Note that during austral spring NIWA-UKCA overestimates CO, presumably  
due to exaggerated tropical biomass burning in the model which causes CO biases of up to 10%  
(Fig. 7b). The sensitivity of OH to changes in CO ( $\frac{\partial \ln[\text{OH}]}{\partial \ln[\text{CO}]}$ ) shown in Fig. 7(f) varies from  $-0.3$  to  
 $-0.5$  and in absolute terms increases with altitude (the white band shown in October is the result of  
CO differences being close to zero).

365 The sensitivities of OH to CH<sub>4</sub> and CO show comparable values at the surface, but the OH sensi-  
tivity to CO increases with height whereas its sensitivity to CH<sub>4</sub> decreases. Note that the CH<sub>4</sub> + OH  
reaction rate is strongly temperature dependent, which may contribute to the lower sensitivity of OH  
to CH<sub>4</sub> changes at altitude than to CO. However, further investigation will need to investigate how  
these ratios change in different chemical regimes, and to assess whether the relative sensitivity of  
370 OH to CO and to CH<sub>4</sub> are specific to the clean Southern-Hemisphere environment.

### 3.4 OH sensitivity to temperature biases

To assess the effects of changes in temperature on OH, we apply the same procedure as for O<sub>3</sub>,  
for which the effects of temperature have been decomposed into kinetics and photolysis effects. We  
perform three simulations: In the first simulation, we only apply temperature changes to chemical  
375 kinetics, keeping all photolysis rates fixed (noting that most uni-, bi-, and termolecular reaction rates  
are temperature dependent). In the second simulation, we only consider the photolysis effect, which  
arises mainly because the cross section of O<sub>3</sub>, the primary UV absorber, is temperature dependent.  
The impact of temperature on OH via ozone photolysis again occurs via two different mechanisms:

380 firstly, the changes in  $j_{O^1D}$  caused by changes in the actinic flux which relates to changes in the atmospheric transmissivity in the UV (caused by a temperature dependence of the cross section of overhead ozone), and the local changes of  $j_{O^1D}$ , due to the local temperature dependence of the ozone cross section. Here, we only evaluate the combined photolysis effect in the second simulation. Finally, we perform a third simulation by applying both the kinetics and the photolysis effects simultaneously.

385 At Lauder, the reference simulation is generally cold-biased (i.e., the temperature correction is positive; fig. 8a). This is particularly the case in the lowest 2 km and throughout the troposphere in the autumn-winter season. The kinetics effect leads to a reduction of OH by up to 2% (fig. 8b).  $O(^1D) + H_2O$  and the quenching reactions (eq. 1) are not or weakly explicitly temperature dependent, making  $CH_4 + OH$  (which is much more sensitive to temperature) the leading factor in causing this small OH reduction. **The rate coefficient for this reaction in NIWA-UKCA and the SCM is  $k_{OH+CH_4} = 1.85 \cdot 10^{-12} \exp(-1690/T)$ ; at 290 K the sensitivity of  $k_{OH+CH_4}$  to temperature changes evaluates to about 2%/K. However, OH is well buffered by other reactions, so its sensitivity is considerably smaller than that.** The photolysis effect is often somewhat larger than the kinetics effect but peaks in spring (fig. 8c). This translates into a slight OH reduction comparable in magnitude to the kinetics effect (fig. 8d). Both effects add nearly completely linearly in the combined simulation (fig. 8e,f).

We calculate sensitivity coefficients  $A_6$  and  $A_6''$  that define the OH responses to both effects (fig. 5 e,f). Coefficient  $A_6$  represents the kinetics effect and varies from 0 to  $-1.75$  (i.e., in absolute terms, the relative OH response can be larger than the relative difference in  $T$ ). The sensitivity coefficient that describes the sensitivity of OH to changes in photolysis ( $A_6''$ ) ranges from 0.6 at the surface to 0 at 10 km of altitude. Figure 5 (e,f) shows sensitivity coefficients for both effects ( $A_6$  and  $A_6''$ ). OH changes due to both effects are small (up to 2.5%) and comparable in magnitude.

Several sensitivity studies have been conducted previously to elucidate the impact of temperature on OH (Stevenson et al., 2000; Wild, 2007; O'Connor et al., 2009). None of these studies separately assessed the impacts of the kinetics and photolysis effects of temperature on OH. Wild (2007) applied a globally uniform temperature rise of 5 K that led to a larger OH abundance and an around 10% decrease in the  $CH_4$  lifetime. O'Connor et al. (2009) showed a small impact on global OH abundances due to temperature biases; this may be because **either** the temperature biases in their model were both positive and negative, in different regions, leading to some cancellation of the impact on global OH, **or to low OH sensitivity to temperature biases**. Here, bias-correcting temperature is shown to **also** have only a small impact on OH abundance (Fig. 8e); this result broadly corroborates that of O'Connor et al. (2009).

### 3.5 Linearity of OH sensitivity to biases in all forcings

Here, we assess the effect of changing all forcings ( $O_3$ ,  $H_2O$ ,  $CH_4$ ,  $CO$ , and temperature) simultaneously on OH at Lauder. Fig. 9(a) shows the responses of OH to changing all forcings. A comparison with fig. 6 suggests that  $H_2O$  changes dominate the total response of OH to changes in these forcings. At Lauder, NIWA-UKCA is too moist (relative to radiosonde water vapour); this translates into a large OH overestimation of up to  $\sim 40\%$  in the reference simulation (Fig. 9a). This is consistent with the underestimated  $CH_4$  lifetime by the NIWA-UKCA model (Morgenstern et al., 2013; Telford et al., 2013), assuming that the NIWA-UKCA model is too moist also in other regions. **(In the NIWA-UKCA reference simulation used here, the global  $CH_4$  lifetime, disregarding dry deposition, is 7.2 years, whereas a recent best estimate is 9.8 years, with an uncertainty range of 7.6 - 14 years (SPARC, 2013)).** In general, in the SCM OH responds approximately linearly to the combined changes in major forcings that play an important role in OH chemistry (Fig. 9).

To examine the linearity of OH responses to simultaneous changes in key forcings defined in this study, the combination of all individual contributions, i.e.  $O_3$  (kinetics and photolysis effects),  $H_2O$ ,  $CH_4$ ,  $CO$ , and temperature (kinetics and photolysis effects) to OH, was compared to the OH response to all forcings combined simulation in the SCM through Eq. (4):

$$\frac{\Delta[OH]}{[OH]_{ref}} \approx A_1 \frac{\Delta[O_3]}{[O_3]_{ref}} + A_1'' \frac{\Delta jO(^1D)_{O_3}}{jO(^1D)_{ref}} + A_2 \frac{\Delta[H_2O]}{[H_2O]_{ref}} + A_4 \frac{\Delta[CH_4]}{[CH_4]_{ref}} + A_5 \frac{\Delta[CO]}{[CO]_{ref}} + A_6 \frac{\Delta T}{T_{ref}} + A_6'' \frac{\Delta jO(^1D)_T}{jO(^1D)_{ref}} \quad (4)$$

where  $\frac{\Delta[OH]}{[OH]_{ref}}$  is the relative difference in the OH concentration obtained with the SCM with respect to the reference simulation, using all forcings combined. The forcings comprise the kinetics and photolysis effects of  $O_3$  ( $A_1$  and  $A_1''$ ), radiosonde  $H_2O$  ( $A_2$ ),  $CH_4$  ( $A_4$ ),  $CO$  ( $A_5$ ), and the kinetics and photolysis effects of temperature ( $A_6$  and  $A_6''$ ). **Eq. 4 expresses a working hypothesis that the model responds linearly to the applied forcings; we will test this assumption in the following paragraph.**

Eq.(4) describes the relationship between the single-perturbation experiments and the all-forcings simulation, assuming that the OH response is linear to changes in the forcings. Figure 9 a,b indicates that the model responds approximately linearly to the combinations of all forcings, with OH responses in the all-forcings simulation correlating at 0.9 with the sum of the OH responses in the individual-forcing simulations. **Fig. 9(c) however also suggests that there are some notable non-linearity in the system chemistry of the troposphere at Lauder. Chemical feedbacks between the impacts of correcting water vapour and ozone may contribute to this non-linearity; for example, a change in the water vapour abundance may impact the sensitivity of OH to changing  $O_3$ .**

### 3.6 Trends in OH

We examine variability and trends in OH using the SCM simulation including all key forcings separately for different altitude bands **bins**. The results (Fig. 10) indicate that there are no significant **long-term** trends in OH throughout the troposphere for the period of the simulation (1994-2010)  
450 **We find trends of  $-2.1 \pm 4.8\%$  at 0-2.5 km,  $0.9 \pm 2.3\%$  at 2.5-5 km,  $2.6 \pm 3.5\%$  at 5-7.5 km, and  $3.6 \pm 4.1\%$  at 7.5-10 km over the period of 1994-2010), but there is evidence substantial interannual variability of interannual variations at all altitudes. This is in agreement with other studies (e.g., Manning et al., 2005; Montzka et al., 2011).**

**In addition, we explore variability and trends in the OH column at Lauder to be compared**  
455 **with other estimates of global OH. As expected from the results of OH trends at different altitude bins, we find no significant long-term trend in the OH column ( $0.5 \pm 1.3\%$ ) (Fig. 11). However, there is evidence of short-term variations (5 – 10%), in agreement with other studies that used observations to infer global OH concentrations (e.g., Manning et al., 2005; Montzka et al., 2011).**

### 460 3.7 OH sensitivity to the presence of clouds

We have assessed the OH sensitivity to correcting biases in key forcings assuming clear **skies**. Here we explore the impact of simulated clouds on OH, recognizing that this process is associated with large uncertainties due to difficulties with representing clouds in models. Measurements of cloud profiles do not exist at Lauder, hence a bias correction like that performed with the composition and  
465 temperature fields is not possible. Therefore, here we only examine the impact of clouds simulated by NIWA-UKCA on  $j_{O^1D}$  and OH at Lauder, relative to the clear-sky reference simulation used before. The impacts of liquid water clouds (LWCs) and ice clouds (ICs) were assessed separately and **combinedly in combination**. Three simulations are defined here, i.e. (1) including only ICs, (2) including only LWCs, and (3) considering both combined (LICs).

470 Fig. 12(a,c,e) shows the response of  $j_{O^1D}$  and OH to the presence of the ICs.  $j_{O^1D}$  and OH are generally reduced below the ICs, relative to the cloud-free situation. The maximum reduction in OH is 10 to 15% in winter below 2 km, coinciding with the maximum reduction in  $j_{O^1D}$ . There are increases in both fields (up to  $\sim 8\%$ ) above the ICs in austral spring, associated with the seasonal peak in IC occurrence at the same time. In general,  $j_{O^1D}$  and OH impacts vary strongly with season,  
475 with the maximum reduction occurring in winter close to the surface, and the maximum increase in spring above the ICs.

LWCs are mostly present between 1 and 4 km with the seasonal peak in austral spring (fig. 12b). Similarly to ICs,  $j_{O^1D}$  and OH are enhanced above and throughout much of the cloud layer, and reduced in the lowest 1 km above the surface (fig. 12e,g). The enhancement in  $j_{O^1D}$  and OH peaks  
480 at 12% between 2 and 4 km of altitude, coinciding with the spring maximum in liquid water content

at 1–2 km. Conversely, the reduction in  $j_{O^1D}$  and OH with respect to the clear-sky condition is  $\sim 10\%$  and is produced below the clouds.

The simulation with the combined effect of ICs and LWCs (LICs) produces a reduction in  $j_{O^1D}$  and OH that ranges between 0% and 20% below the transition of ICs to LWCs at around 2 km, since  
485 LWCs are as much as twice as optically dense as ICs (fig. 12g). An enhancement is produced above this altitude of up to 18%. The magnitudes of changes in  $j_{O^1D}$  and OH are similar when either ICs or LWCs are considered in the SCM. Furthermore, their effects add up slightly less than linearly when both are present in the simulations (fig. 12h).

The results shown here indicate that lower clouds generally produce an enhancement in  $j_{O^1D}$   
490 (Fig. 12d), but higher clouds generally produce a reduction in  $j_{O^1D}$  in the free troposphere (Fig. 12b; Tang et al., 2003; Tie et al., 2003; Liu et al., 2009). Furthermore, the vertically and seasonally averaged enhancement and reduction in  $j_{O^1D}$  are about 2% and 6% respectively for the LWC clouds, similar to the response for the ICs condition; this suggests that the cloud vertical distribution has a bigger effect on photolysis than the change in cloud water content (Tie et al., 2003).

#### 495 4 Conclusions

The sensitivity of the OH abundance at Lauder to NIWA-UKCA model biases in key forcing variables ( $O_3$ ,  $H_2O$ ,  $CH_4$ ,  $CO$ , and temperature) have been quantified for clear-sky conditions, using a single-column model (SCM). Only fast photochemistry is represented in the SCM; slow chemistry  
500 (i.e. timescales similar to or longer than the 1-hour chemical timestep), transport, and other physical processes are thus not considered. The bias-corrected profiles of the key forcing variables have been constructed largely using long-term Lauder measurements, combined with NIWA-UKCA output. Also a few other sources of data (Cape Grim methane measurements, ERA-Interim water vapour) have been used.

The results show that OH responds approximately linearly to correcting biases in  $O_3$ ,  $H_2O$ ,  $CH_4$ ,  
505  $CO$ , and temperature. We have decomposed the OH response to  $O_3$  changes into the kinetic effect (i.e. local impacts on the chemical equilibrium steady state of changing  $[O_3]$ ) and the photolysis effect (as mediated by changes in the overhead  $O_3$  column affecting photolysis rates). We find that the kinetic effect of correcting positive biases in modelled  $O_3$  causes a reduction in OH during austral summer and autumn (by up to 20% at 7 km), and an increase in the free troposphere in  
510 austral spring (of  $> 5\%$  in October at 3 km); such changes in OH are nearly linearly related to the corresponding ozone biases. NIWA-UKCA generally overestimates the ozone column. Correcting this effect bias causes  $j_{O^1D}$  to increase by 15 – 30% below 10 km, causing general OH increases which maximize at around 16% between 2 and 6 km in summer. The model responds approximately linearly to the combined effects of photolysis and kinetics.

515 NIWA-UKCA considerably overestimates the H<sub>2</sub>O vapour concentration **by up to ~ 50%** compared to radiosonde measurements. Correcting this moist bias leads to > 34% reductions in OH in the free troposphere during the austral summer. The sensitivity coefficient of OH to biases in H<sub>2</sub>O vapour is relatively large in the lower troposphere but decreases with altitude. Assuming this moist bias is not restricted to Lauder (which we do not assess here), this is thus a leading explanation  
520 for NIWA-UKCA to produce an underestimated CH<sub>4</sub> lifetime (**Morgenstern et al., 2013; Telford et al., 2013**), relative to accepted literature estimates (**Naik et al., 2013; Voulgarakis et al., 2013; SPARC, 2013**).

The bias in modelled CH<sub>4</sub> is small since surface CH<sub>4</sub> in the SCM reference simulation is constrained to follow globally averaged surface observations. The Southern Hemisphere generally has a  
525 slightly smaller CH<sub>4</sub> burden than the North. Correcting the resulting positive bias at Lauder causes increases in OH throughout the troposphere, with a seasonal peak in March/April. OH is most sensitive to CH<sub>4</sub> changes in winter, though. In the analysis of the OH sensitivity to CH<sub>4</sub>, the impact of subsequent changes in CH<sub>4</sub> oxidation products which also affect OH could not be addressed within the constraints of an SCM. Inclusion of this effect could change the sensitivity coefficient for CH<sub>4</sub>  
530 (Spivakovsky et al., 2000).

Except for October-December, NIWA-UKCA has a tendency to underestimate CO. As with CH<sub>4</sub>, the sensitivity of OH to changes in CO is negative throughout the troposphere, reflecting that CO + OH is an important sink for OH.

We show that OH responds linearly to temperature biases. These effects cause a small reduction in  
535 OH due to the strong dependence of OH + CH<sub>4</sub> on temperature (eq. 1). However, ~~for NIWA-UKCA the impact of temperature biases impact on OH at Lauder is small,~~ **the impact of this reaction on OH is buffered by other less temperature-dependent reactions, causing only a small sensitivity of OH to temperature. This is** in agreement with O'Connor et al. (2009).

The results of the simulation considering simultaneous changes in all the key forcings indicate that  
540 OH responds approximately linearly to all the major forcings that contribute to the oxidising capacity of the atmosphere. We find that biases in O<sub>3</sub>, H<sub>2</sub>O, CH<sub>4</sub>, CO, and temperature all affect the oxidising capacity of the atmosphere at Lauder, with H<sub>2</sub>O and O<sub>3</sub> biases dominating. ~~The NIWA-UKCA model generally produces a moist bias (by ~ 0–50%) relative to radiosonde measurements; this leads to an overestimation of OH of up to 40%. This makes water vapour a leading contender~~  
545 ~~to explain the underestimated global lifetime of CH<sub>4</sub> in NIWA-UKCA (Morgenstern et al., 2013; Telford et al., 2013).~~ We find no significant trend in OH over Lauder over the period 1994-2010.

The SCM approach can be applied to other parts of the globe where reliable long-term observations of O<sub>3</sub> and H<sub>2</sub>O exist. In-situ observations of CH<sub>4</sub> and CO are not that critical; CH<sub>4</sub> can be estimated from non-local measurements, and relatively reliable satellite measurements of total-column CO exist (e.g., Pan et al., 1995; Morgenstern et al., 2012). However, in polluted regions, such  
550 as in much of the Northern Hemisphere, NO<sub>x</sub> and NMVOC levels are elevated relative to Lauder and

affect in situ ozone production. This means that these constituents might need to be bias-corrected if the SCM is applied in such regions. This might affect the suitability of our approach under these conditions.

555 Having determined the contributions of the major forcings to the chemistry of OH at Lauder under clear-sky conditions, a step forward would be to assess the impact of clouds on photolysis and thus OH, which could be substantial. Due to a lack of suitable observations to constrain the SCM model with cloud profiles at Lauder, we only assessed how the presence of modelled cloud affects OH, relative to the clear-sky situation. The results show that OH response to cloud strongly depends on  
560 the vertical distribution of the clouds, not just the total amount. Both liquid- and ice clouds lead to increases in OH above and to some extent inside the cloud, particularly in the spring season when this effect maximizes. Considering that clouds are amongst the most difficult aspects of the climate system to model adequately, we stipulate that observational profiles of cloud properties would be highly desirable to use for a future continuation of this line of research.

565 In summary, we conclude that at Lauder, OH modelled in NIWA-UKCA is most sensitive to issues with representing water vapour and ozone. This points to the need to improve representations of the hydrological cycle and of tropospheric and stratospheric ozone chemistry in NIWA-UKCA and possibly other, similar chemistry-climate models. **Water vapour is coupled to clouds in NIWA-UKCA; it is well known that clouds are difficult to represent adequately in global  
570 low-resolution climate models. The biases in ozone may well be partly caused by the moist bias in NIWA-UKCA; this is a subject of ongoing research.**

**Progress with the simulation of the hydrological cycle in present-generation Earth System Models should improve the simulated water vapour product. Simulating an accurate hydro-  
575 logical cycle has been a long-standing issue in climate models, and progress has been slow. If errors in the simulation of moisture cannot be avoided, perhaps their impact on OH can be corrected for using an approach similar to that which we have presented but using global water vapour measurements. Such a "correction" of modelled OH might result in a reduction in the inter-model spread of the OH abundance and consequently a more accurate quantification of the methane lifetime. For this, tropical radiosonde data would be particularly valuable – most  
580 OH is located in the tropics (SPARC, 2013). A similar approach could be used to account of the influence of errors in ozone, although tropospheric in situ ozone measurements may be too sparse to allow for a sufficient characterization of the error in models.**

#### **Author contributions**

O. Morgenstern devised the original idea. L. López Comí wrote the model, conducted the simula-  
585 tions, performed the data analysis, and led the writing of the paper, with support from S. Masters, O.

Morgenstern, and G. Zeng. G. Nedoluha contributed the microwave ozone data to the research; R. Querel contributed the ozone sonde data. All authors contributed to the writing of the manuscript.

*Acknowledgements.* All data used in this paper can be obtained from the contact author. This work has been supported by NIWA as part of its Government-funded, core research from New Zealand's Ministry of Business, Innovation, and Employment (MBIE). We would like to thank the Lauder team for providing most of the measurements used here. We particularly thank Dan Smale for his help with various aspects of this work. We acknowledge NOAA for the FPH data. We acknowledge ECMWF for provision of the ERA-Interim data **and NOAA/OAR/ESRL PSD, Boulder, Colorado, USA, for provision of the NCEP/NCAR reanalyses.** We acknowledge CSIRO Marine and Atmospheric Research and the Australian Bureau of Meteorology for the Cape Grim methane measurements. CSIRO and the Australian Bureau of Meteorology give no warranty regarding the accuracy, completeness, currency or suitability for any particular purpose and accept no liability in respect of data. We acknowledge the U.K. Met Office for use of the MetUM. Furthermore, we acknowledge the contribution of NeSI high-performance computing facilities to the results of this research. NZ's national facilities are provided by the NZ eScience Infrastructure and funded jointly by NeSI's collaborator institutions and through MBIE's Infrastructure programme (<https://www.nesi.org.nz>).

## References

- Badosa, J., McKenzie, R. L., Kotkamp, M., Calbó, J., González, J. A., Johnston, P. V., O'Neill, M., and Anderson, D. J.: Towards closure between measured and modelled UV under clear skies at four diverse sites, *Atmos. Chem. Phys.*, 7, 2817–2837, doi:10.5194/acp-7-2817-2007, 2007.
- 605 Bergman, J. and Sardeshmukh, P.: Dynamic stabilization of atmospheric single column models, *J. Climate*, 17, 1004–1021, 2004.
- Bloss, W. J., Lee, J. D., Heard, D. E., Salmon, R. A., Bauguutte, S. J. B., Roscoe, H. K., and Jones, A. E.: Observations of OH and HO<sub>2</sub> radicals in coastal Antarctica, *Atmos. Chem. Phys.*, 7, 4171–4185, doi:10.5194/acp-7-4171-2007, <http://www.atmos-chem-phys.net/7/4171/2007/>, 2007.
- 610 Bodeker, G. E., Boyd, I. S., and Matthews, W. A.: Trends and variability in vertical ozone and temperature profiles measured by ozonesondes at Lauder, New Zealand: 1986–1996, *J. Geophys. Res. Atmos.*, 103, 28,661–28,681, 1998.
- Bousquet, P., Hauglustaine, D. A., Peylin, P., Carouge, C., and Ciais, P.: Two decades of OH variability as inferred by an inversion of atmospheric transport and chemistry of methyl chloroform, *Atmos. Chem. Phys.*,
- 615 5, 2635–2656, doi:10.5194/acp-5-2635-2005, 2005.
- Boyd, I. S., Parrish, A. D., Froidevaux, L., von Clarmann, T., Kyrölä, E., Russell III, J. M., and Zawodny, J. M.: Ground-based microwave ozone radiometer measurements compared with Aura-MLS v2.2 and other instruments at two Network for Detection of Atmospheric Composition Change sites, *J. Geophys. Res. Atmos.*, 112, doi:10.1029/2007JD008720, 2007.
- 620 Carver, G., Brown, P., and Wild, O.: The ASAD atmospheric chemistry integration package and chemical reaction database, *Comput. Phys. Commun.*, 105, 197–215, doi:10.1016/S0010-4655(97)00056-8, 1997.
- Creasey, D., Evans, G., Heard, D., and Lee, J.: Measurements of OH and HO<sub>2</sub> concentrations in the Southern Ocean marine boundary layer, *J. Geophys. Res. Atmos.*, 108, 4475, 2003.
- Cunnold, D. and et al.: In situ measurements of atmospheric methane at GAGE/AGAGE sites during 1985–2000
- 625 and resulting source inferences, *J. Geophys. Res. Atmos.*, 107, 4225, 2002.
- Cuxart, J., Holtzlag, A., Beare, R., Bazile, E., Beljaars, A., Cheng, A., Conangla, L., Ek, M., Freedman, F., Hamdi, R., Kerstein, A., Kitagawa, H., Lenderink, G., Lewellen, D., Mailhot, J., Mauritsen, T., Perov, V., Schayes, G., Steeneveld, G., Svensson, G., Taylor, P., Weng, W., Wunsch, S., and Xu, K.: Single-column model intercomparison for a stably stratified atmospheric boundary layer, *Bound.-Layer Meteor.*, 118, 273–
- 630 303, 2006.
- Dal Gesso, S., van der Dussen, J. J., Siebesma, A. P., de Roode, S. R., Boutle, I. A., Kamae, Y., Roehrig, R., and Vial, J.: A single-column model intercomparison on the stratocumulus representation in present-day and future climate, *J. Adv. Mod. Earth Systems*, 7, 617–647, doi:10.1002/2014MS000377, 2015.
- Dee, D. P. and et al.: The ERA-Interim reanalysis: configuration and performance of the data assimilation
- 635 system, *Quart. J. Royal Meteorol. Soc.*, 137, 553–597, 2011.
- DeMore, W. B.: Experimental and estimated rate constants for the reactions of hydroxyl radicals with several halocarbons, *JPC*, 100, 5813–5820, doi:10.1021/jp953216+, 1996.
- Dentener, F., Peters, W., Krol, M., van Weele, M., Bergamaschi, P., and Lelieveld, J.: Interannual variability and trend of CH<sub>4</sub> lifetime as a measure for OH changes in the 1979–1993 time period, *J. Geophys. Res. Atmos.*,
- 640 108, doi:10.1029/2002JD002916, 4442, 2003.

- Dusanter, S., Vimal, D., Stevens, P. S., Volkamer, R., and Molina, L. T.: Measurements of OH and HO<sub>2</sub> concentrations during the MCMA–2006 field campaign – Part 1: Deployment of the Indiana University laser-induced fluorescence instrument, *Atmos. Chem. Phys.*, 9, 1665–1685, 2009.
- 645 Elshorbany, Y. F., Kleffmann, J., Hofzumahaus, A., Kurtenbach, R., Wiesen, P., Brauers, T., Bohn, B., Dorn, H.-P., Fuchs, H., Holland, F., Rohrer, F., Tillmann, R., Wegener, R., Wahner, A., Kanaya, Y., Yoshino, A., Nishida, S., Kajii, Y., Martinez, M., Kubistin, D., Harder, H., Lelieveld, J., Elste, T., Plass-Dülmer, C., Stange, G., Berresheim, H., and Schurath, U.: HO<sub>x</sub> budgets during HO<sub>x</sub>Comp: A case study of HO<sub>x</sub> chemistry under NO<sub>x</sub>-limited conditions, *J. Geophys. Res. Atmos.*, 117, n/a–n/a, doi:10.1029/2011JD017008, D03307, 2012.
- 650 Emmerson, K., Carslaw, N., Carpenter, L., Heard, D., Lee, J., and Pilling, M.: Urban atmospheric chemistry during the PUMA campaign 1: Comparison of modelled OH and HO<sub>2</sub> concentrations with measurements, *J. Atmos. Chem.*, 52, 143–164, 2005.
- Emmerson, K. M., Carslaw, N., Carslaw, D. C., Lee, J. D., McFiggans, G., Bloss, W. J., Gravestock, T., Heard, D. E., Hopkins, J., Ingham, T., Pilling, M. J., Smith, S. C., Jacob, M., and Monks, P. S.: Free radical modelling studies during the UK TORCH campaign in summer 2003, *Atmos. Chem. Phys.*, 7, 167–181, doi:10.5194/acp-7-167-2007, <http://www.atmos-chem-phys.net/7/167/2007/>, 2007.
- 655 Eyring, V. and et al.: Overview of IGAC/SPARC Chemistry–Climate Model Initiative (CCMI) community simulations in support of upcoming ozone and climate assessments, *SPARC Newsletter*, 40, 48–66, 2013.
- Fuglestad, J., Jonson, J., and Isaksen, I.: Effects of reductions in stratospheric ozone on tropospheric chemistry through changes in photolysis rates, *Tellus B Chem. Phys. Meteor.*, 46B, 172–192, 1994.
- 660 Hall, E. G., Jordan, A. F., Hurst, D. F., Oltmans, S. J., Vömel, H., Kühnreich, B., and Ebert, V.: Advancements, measurement uncertainties, and recent comparisons of the NOAA frostpoint hygrometer, *Atmos. Meas. Tech. Discuss.*, doi:10.5194/amt-2016-160, 2016.
- Heard, D. E. and Pilling, M. J.: Measurement of OH and HO<sub>2</sub> in the troposphere, *Chem. Rev.*, 103, 5163–5198, 665 2003.
- Hess, P. and Mahowald, N.: Interannual variability in hindcasts of atmospheric chemistry: the role of meteorology, *Atmos. Chem. Phys.*, 9, 5261–5280, doi:10.5194/acp-9-5261-2009, 2009.
- Holmes, C. D., Prather, M. J., Søvde, O. A., and Myhre, G.: Future methane, hydroxyl, and their uncertainties: key climate and emission parameters for future predictions, *Atmos. Chem. Phys.*, 13, 285–302, 670 doi:10.5194/acp-13-285-2013, 2013.
- John, J. G., Fiore, A. M., Naik, V., Horowitz, L. W., and Dunne, J. P.: Climate versus emission drivers of methane lifetime against loss by tropospheric OH from 1860–2100, *Atmos. Chem. Phys.*, 12, 12021–12036, doi:10.5194/acp-12-12021-2012, 2012.
- Johnson, C. E., Stevenson, D. S., Collins, W. J., and Derwent, R. G.: Role of climate feedback on methane and ozone studied with a Coupled Ocean–Atmosphere–Chemistry Model, *Geophys. Res. Lett.*, 28, 1723–1726, 675 doi:10.1029/2000GL011996, 2001.
- Joyce, P. L., von Glasow, R., and Simpson, W. R.: The fate of NO<sub>x</sub> emissions due to nocturnal oxidation at high latitudes: 1–D simulations and sensitivity experiments, *Atmos. Chem. Phys.*, 14, 7601–7616, doi:10.5194/acp-14-7601-2014, 2014.

- 680 Kalnay, E., Kanamitsu, M., Kistler, R., Collins, W., Deaven, D., Gandin, L., Iredell, M., Saha, S., White, G.,  
Woolen, J., Zhu, Y., Chelliah, M., Ebisuzaki, W., Higgins, W., Janowiak, J., Mo, K., Ropelewski, C., Wang,  
J., Leetmaa, A., Reynolds, R., Jenne, R., and Joseph, D.: The NCEP/NCAR 40-year reanalysis project, *Bull.*  
*Amer. Meteorol. Soc.*, *77*, 437–470, 1996.
- Krol, M. C., Meirink, J. F., Bergamaschi, P., Mak, J. E., Lowe, D., Jöckel, P., Houweling, S., and Röckmann,  
685 T.: What can  $^{14}\text{C}$ O measurements tell us about OH?, *Atmos. Chem. Phys.*, *8*, 5033–5044, doi:10.5194/acp-  
8-5033-2008, 2008.
- Kylling, A., Webb, A., Kift, R., Gobbi, G., Ammannato, L., Barnaba, F., Bais, A., Kazadzis, S., Wendisch, M.,  
Jakel, E., Schmidt, S., Kniffka, A., Thiel, S., Junkermann, W., Blumthaler, M., Silbernagl, R., Schallhart,  
B., Schmitt, R., Kjeldstad, B., Thorseth, T., Scheirer, R., and Mayer, B.: Spectral actinic flux in the lower  
690 troposphere: measurement and 1-D simulations for cloudless, broken cloud and overcast situations, *Atmos.*  
*Chem. Phys.*, *5*, 1975–1997, 2005.
- Lebassi-Habtezion, B. and Caldwell, P. M.: Aerosol specification in single-column Community Atmosphere  
Model version 5, *Geosci. Model Dev.*, *8*, 817–828, doi:10.5194/gmd-8-817-2015, 2015.
- Lelieveld, J. and Dentener, F. J.: What controls tropospheric ozone?, *J. Geophys. Res. Atmos.*, *105*, 3531–3551,  
695 doi:10.1029/1999jd901011, 2000.
- Lelieveld, J., Crutzen, P. J., and Dentener, F. J.: Changing concentration, lifetime and climate forcing of atmo-  
spheric methane, *Tellus B Chem. Phys. Meteor.*, *50*, 128–150, doi:10.1034/j.1600-0889.1998.t01-1-00002.x,  
1998.
- Lelieveld, J., Dentener, F. J., Peters, W., and Krol, M. C.: On the role of hydroxyl radicals in the self-cleansing  
700 capacity of the troposphere, *Atmos. Chem. Phys.*, *4*, 2337–2344, doi:10.5194/acp-4-2337-2004, 2004.
- Levy, H.: Normal atmosphere: Large radical and formaldehyde concentrations predicted, *Science*, *173*, 141–  
143, 1971.
- Liu, H., Crawford, J. H., Considine, D. B., Platnick, S., Norris, P. M., Duncan, B. N., Pierce, R. B., Chen, G.,  
and Yantosca, R. M.: Sensitivity of photolysis frequencies and key tropospheric oxidants in a global model  
705 to cloud vertical distributions and optical properties, *J. Geophys. Res. Atmos.*, *114*, d10305, 2009.
- Liu, S. C. and Trainer, M.: Response of the tropospheric ozone and odd hydrogen radicals to column ozone  
change, *J. Atmos. Chem.*, *6*, 221–233, 1988.
- Logan, J. A., Prather, M. J., Wofsy, S. C., and McElroy, M. B.: Tropospheric chemistry: A global perspective,  
*J. Geophys. Res. Oceans*, *86*, 7210–7254, doi:10.1029/jc086ic08p07210, 1981.
- 710 López Comí, L.: Single-column model analysis of available NIWA observations to determine the self-cleaning  
capacity of the atmosphere, PhD thesis, U. Canterbury, Christchurch, 2016.
- Madronich, S. and Granier, C.: Impact of recent total changes on tropospheric ozone photodissociation, hy-  
droxyl radicals, and methane trends, *Geophys. Res. Lett.*, *19*, 465–467, 1992.
- Manning, M., Lowe, D., Moss, R., Bodeker, G., and Allan, W.: Short-term variations in the oxidizing power of  
715 the atmosphere, *Nature*, *436*, 1001–1004, 2005.
- McKenzie, R. L., Weinreis, C., Johnston, P. V., Liley, B., Shiona, H., Kotkamp, M., Smale, D., Takegawa, N.,  
and Kondo, Y.: Effects of urban pollution on UV spectral irradiances, *Atmos. Chem. Phys.*, *8*, 5683–5697,  
doi:10.5194/acp-8-5683-2008, 2008.

- Meinshausen, M., Smith, S. J., Calvin, K. V., Daniel, J. S., Kainuma, M. L. T., Lamarque, J.-F., Matsumoto, K., Montzka, S., Raper, S., Riahi, K., Thomson, A. M., Velders, G. J. M., and van Vuuren, D. P.: The RCP greenhouse gas concentrations and their extensions from 1765 to 2300, *Climatic Change*, 109, 213–241, doi:10.1007/s10584-011-0156-z, 2011.
- Mihailovic, D., Rao, S., Alapaty, K., Ku, J., Arsenic, I., and Lalic, B.: A study on the effects of subgrid-scale representation of land use on the boundary layer evolution using a 1-D model, *Environ. Mod. Soft.*, 20, 705–714, doi:10.1016/j.envsoft.2004.04.004, 2005.
- Miloshevich, L., Vomel, H., Paukkunen, A., Heymsfield, A., and Oltmans, S.: Characterization and correction of relative humidity measurements from vaisala RS80-A radiosondes at cold temperatures, *J. Atmos. Ocean. Technol.*, 18, 135–156, 2001.
- Montzka, S. A., Krol, M., Dlugokencky, E., Hall, B., Jöckel, P., and Lelieveld, J.: Small Interannual Variability of Global Atmospheric Hydroxyl, *Science*, 331, 67–69, 2011.
- Morgenstern, O., Braesicke, P., O'Connor, F. M., Bushell, A. C., Johnson, C. E., Osprey, S. M., and Pyle, J. A.: Evaluation of the new UKCA climate-composition model – Part 1: The stratosphere, *Geosci. Model Dev.*, 2, 43–57, doi:10.5194/gmd-2-43-2009, 2009.
- Morgenstern, O., Zeng, G., Wood, S. W., Robinson, J., Smale, D., Paton-Walsh, C., Jones, N. B., and Griffith, D. W. T.: Long-range correlations in Fourier transform infrared, satellite, and modeled CO in the Southern Hemisphere, *J. Geophys. Res.*, 117, doi:10.1029/2012JD017639, 2012.
- Morgenstern, O., Zeng, G., Abraham, N. L., Telford, P. J., Braesicke, P., Pyle, J. A., Hardiman, S. C., O'Connor, F. M., and Johnson, C. E.: Impacts of climate change, ozone recovery, and increasing methane on surface ozone and the tropospheric oxidizing capacity, *J. Geophys. Res. Atmos.*, 118, 1028–1041, doi:10.1029/2012JD018382, 2013.
- Morgenstern, O., Hegglin, M. I., Rozanov, E., O'Connor, F. M., Abraham, N. L., Akiyoshi, H., Archibald, A. T., Bekki, S., Butchart, N., Chipperfield, M. P., Deushi, M., Dhomse, S. S., Garcia, R. R., Hardiman, S. C., Horowitz, L. W., Jöckel, P., Josse, B., Kinnison, D., Lin, M. Y., Mancini, E., Manyin, M. E., Marchand, M., Marécal, V., Michou, M., Oman, L. D., Pitari, G., Plummer, D. A., Revell, L. E., Saint-Martin, D., Schofield, R., Stenke, A., Stone, K., Sudo, K., Tanaka, T. Y., Tilmes, S., Yamashita, S., Yoshida, Y., and Zeng, G.: Review of the global models used within the Chemistry-Climate Model Initiative (CCMI), *Geosci. Model Dev. Discuss*, doi:10.5194/gmd-2016-199, 2016.
- Naik, V., Voulgarakis, A., Fiore, A. M., Horowitz, L. W., Lamarque, J.-F., Lin, M., Prather, M. J., Young, P. J., Bergmann, D., Cameron-Smith, P. J., Cionni, I., Collins, W. J., Dalsøren, S. B., Doherty, R., Eyring, V., Faluvegi, G., Folberth, G. A., Josse, B., Lee, Y. H., MacKenzie, I. A., Nagashima, T., van Noije, T. P. C., Plummer, D. A., Righi, M., Rumbold, S. T., Skeie, R., Shindell, D. T., Stevenson, D. S., Strode, S., Sudo, K., Szopa, S., and Zeng, G.: Preindustrial to present-day changes in tropospheric hydroxyl radical and methane lifetime from the Atmospheric Chemistry and Climate Model Intercomparison Project (ACCMIP), *Atmos. Chem. Phys.*, 13, 5277–5298, doi:10.5194/acp-13-5277-2013, 2013.
- Nedoluha, G. E., Boyd, I. S., Parrish, A., Gomez, R. M., Allen, D. R., Froidevaux, L., Connor, B. J., and Querel, R. R.: Unusual stratospheric ozone anomalies observed in 22 years of measurements from Lauder, New Zealand, *Atmos. Chem. Phys.*, 15, 6817–6826, doi:10.5194/acp-15-6817-2015, 2015.

- 760 Neu, J. L., Prather, M. J., and Penner, J. E.: Global atmospheric chemistry: Integrating over fractional cloud cover, *J. Geophys. Res. Atmos.*, 112, n/a–n/a, doi:10.1029/2006JD008007, <http://dx.doi.org/10.1029/2006JD008007>, D11306, 2007.
- O'Connor, F. M., Johnson, C. E., Morgenstern, O., Abraham, N. L., Braesicke, P., Dalvi, M., Folberth, G. A., Sanderson, M. G., Telford, P. J., Voulgarakis, A., Young, P. J., Zeng, G., Collins, W. J., and Pyle, J. A.: Evaluation of the new UKCA climate-composition model – Part 2: The Troposphere, *Geosci. Model Dev.*, 7, 41–91, doi:10.5194/gmd-7-41-2014, <http://www.geosci-model-dev.net/7/41/2014/>, 2014.
- 765 O'Connor, F. M., Johnson, C. E., Morgenstern, O., and Collins, W. J.: Interactions between tropospheric chemistry and climate model temperature and humidity biases, *Geophys. Res. Lett.*, 36, L16801, 2009.
- Organization, W. M.: Scientific Assessment of Ozone Depletion: 2010, vol. 52, Global Ozone Research and Monitoring Project, 516pp, 2011.
- 770 Pan, L., Edwards, D. P., Gille, J. C., Smith, M. W., and Drummond, J. R.: Satellite remote sensing of tropospheric CO and CH<sub>4</sub>: forward model studies of the MOPITT instrument, *Appl. Opt.*, 34, 6976–6988, doi:10.1364/AO.34.006976, 1995.
- Piot, M. and von Glasow, R.: The potential importance of frost flowers, recycling on snow, and open leads for ozone depletion events, *Atmos. Chem. Phys.*, 8, 2437–2467, 2008.
- 775 Pöschl, U., von Kuhlmann, R., Poisson, N., and Crutzen, P. J.: Development and Intercomparison of Condensed Isoprene Oxidation Mechanisms for Global Atmospheric Modeling, *J. Atmos. Chem.*, 37, 29–52, 2000.
- Prinn, R., Huang, J., Weiss, R., Cunnold, D., Fraser, P., Simmonds, P., McCulloch, A., Harth, C., Reimann, S., Salameh, P., O'Doherty, S., Wang, R., Porter, L., Miller, B., and Krummel, P.: Evidence for variability of atmospheric hydroxyl radicals over the past quarter century, *Geophys. Res. Lett.*, 32, L07809, 2005.
- 780 Prinn, R. G.: Evidence for substantial variations of atmospheric hydroxyl radicals in the past two decades, *Science*, 293, 1048, 2001.
- Randall, D., Krueger, S., Bretherton, C., Curry, J., Duynkerke, P., Moncrieff, M., Ryan, B., Starr, D., Miller, M., Rossow, W., Tselioudis, G., and Wielicki, B.: Confronting models with data – The GEWEX cloud systems study, *Bull. Amer. Meteor. Soc.*, 84, 455–469, 2003.
- 785 Rayner, N. A., Parker, D. E., Horton, E. B., Folland, C. K., Alexander, L. V., Rowell, D. P., Kent, E. C., and Kaplan, A.: Global analyses of sea surface temperature, sea ice, and night marine air temperature since the late nineteenth century, *J. Geophys. Res.*, 108, 4407, doi:10.1029/2002JD002670, 2003.
- Ren, X., Harder, H., Martinez, M., Leshner, R. L., Olinger, A., Simpas, J. B., Brune, W. H., Schwab, J. J., Demerjian, K. L., He, Y., Zhou, X., and Gao, H.: OH and HO<sub>2</sub> chemistry in the urban atmosphere of New York City, *Atmos. Environ.*, 37, 3639–3651, 2003.
- 790 Rinsland, C., Jones, N., Connor, B., Logan, J., Pougatchev, N., Goldman, A., Murcray, F., Stephen, T., Pine, A., Zander, R., Mahieu, E., and Demoulin, P.: Northern and southern hemisphere ground-based infrared spectroscopic measurements of tropospheric carbon monoxide and ethane, *J. Geophys. Res. Atmos.*, 103, 28 197–28 217, 1998.
- 795 Shindell, D. T., Faluvegi, G., Unger, N., Aguilar, E., Schmidt, G. A., Koch, D. M., Bauer, S. E., and Miller, R. L.: Simulations of preindustrial, present-day, and 2100 conditions in the NASA GISS composition and climate model G-PUCCINI, *Atmos. Chem. Phys.*, 6, 4427–4459, doi:10.5194/acp-6-4427-2006, 2006.

- SPARC: SPARC Report on the Lifetimes of Stratospheric Ozone-Depleting Substances, Their Replacements, and Related Species, SPARC Report, 6, WCRP-15/2013, 2013.
- 800 Spivakovsky, C. M., Logan, J. A., Montzka, S. A., Balkanski, Y. J., Foreman-Fowler, M., Jones, D. B. A., Horowitz, L. W., Fusco, A. C., Brenninkmeijer, C. A. M., Prather, M. J., Wofsy, S. C., and McElroy, M. B.: Three-dimensional climatological distribution of tropospheric OH: Update and evaluation, *J. Geophys. Res. Atmos.*, 105, 8931–8980, 2000.
- Stedman, D. H. and McEwan, M. J.: Oxides of nitrogen at two sites in New Zealand, *Geophys. Res. Lett.*, 10, 168–171, doi:10.1029/GL010i002p00168, 1983.
- 805 Stevenson, D., Johnson, C., Collins, W., Derwent, R., and Edwards, J.: Future estimates of tropospheric ozone radiative forcing and methane turnover – the impact of climate change, *Geophys. Res. Lett.*, 27, 2073–2076, 2000.
- Stevenson, D., Dentener, F., Schultz, M., Ellingsen, K., van Noije, T., Wild, O., Zeng, G., Amann, M., Atherton, C., Bell, N., Bergmann, D., Bey, I., Butler, T., Cofala, J., Collins, W., Derwent, R., Doherty, R., Drevet, 810 J., Eskes, H., Fiore, A., Gauss, M., Hauglustaine, D., Horowitz, L., Isaksen, I., Krol, M., Lamarque, J., Lawrence, M., Montanaro, V., Müller, J., Pitari, G., Prather, M., Pyle, J., Rast, S., Rodriguez, J., Sanderson, M., Savage, N., Shindell, D., Strahan, S., Sudo, K., and Szopa, S.: Multimodel ensemble simulations of present-day and near-future tropospheric ozone, *J. Geophys. Res. Atmos.*, 111, D08301, 2006.
- Stone, K. A., Morgenstern, O., Karoly, D. J., Klekociuk, A. R., French, W. J., Abraham, N. L., and Schofield, R.: 815 Evaluation of the ACCESS – chemistry–climate model for the Southern Hemisphere, *Atmos. Chem. Phys.*, 16, 2401–2415, doi:10.5194/acp-16-2401-2016, 2016.
- Tang, Y., Carmichael, G. R., Uno, I., Woo, J.-H., Kurata, G., Lefer, B., Shetter, R. E., Huang, H., Anderson, B. E., Avery, M. A., Clarke, A. D., and Blake, D. R.: Impacts of aerosols and clouds on photolysis frequencies and photochemistry during TRACE-P: 2. Three-dimensional study using a regional chemical transport 820 model, *J. Geophys. Res. Atmos.*, 108, 8822, 2003.
- Telford, P. J., Abraham, N. L., Archibald, A. T., Braesicke, P., Dalvi, M., Morgenstern, O., O’Connor, F. M., Richards, N. A. D., and Pyle, J. A.: Implementation of the Fast-JX Photolysis scheme (v6.4) into the UKCA component of the MetUM chemistry–climate model (v7.3), *Geosci. Model Dev.*, 6, 161–177, doi:10.5194/gmd-6-161-2013, 2013.
- 825 Thompson, A. M.: The oxidizing capacity of the Earth’s atmosphere: Probable past and future changes, *Science*, 256, 1157–1165, 1992.
- Thompson, A. M., Stewart, R. W., Owens, M. A., and Herwehe, J. A.: Sensitivity of tropospheric oxidants to global chemical and climate change, *Atmos. Environ.*, 23, 519–532, 1989.
- Tie, X., Madronich, S., Walters, S., Zhang, R., Rasch, P., and Collins, W.: Effect of clouds on photolysis and 830 oxidants in the troposphere, *J. Geophys. Res. Atmos.*, 108, 4642, 2003.
- Vömel, H., David, D. E., , and Smith, K.: Accuracy of tropospheric and stratospheric water vapor measurements by the cryogenic frost point hygrometer: Instrumental details and observations, *J. Geophys. Res.*, 112, doi:10.1029/2006JD007224, 8305, 2007.
- Voulgarakis, A., Naik, V., Lamarque, J.-F., Shindell, D. T., Young, P. J., Prather, M. J., Wild, O., Field, R. D., 835 Bergmann, D., Cameron-Smith, P., Cionni, I., Collins, W. J., Dalsøren, S. B., Doherty, R. M., Eyring, V., Faluvegi, G., Folberth, G. A., Horowitz, L. W., Josse, B., MacKenzie, I. A., Nagashima, T., Plummer, D. A.,

- Righi, M., Rumbold, S. T., Stevenson, D. S., Strode, S. A., Sudo, K., Szopa, S., and Zeng, G.: Analysis of present day and future OH and methane lifetime in the ACCMIP simulations, *Atmos. Chem. Phys.*, 13, 2563–2587, doi:10.5194/acp-13-2563-2013, 2013.
- 840 Vupputuri, R., Higuchi, K., and Hengeveld, H.: A 1–D modelling of climatic and chemical effects of greenhouse gases, *Theor. Appl. Climatol.*, 52, 151–167, doi:10.1007/BF00864039, 1995.
- Wild, O.: Modelling the global tropospheric ozone budget: exploring the variability in current models, *Atmos. Chem. Phys.*, 7, 2643–2660, 2007.
- Wild, O. and Palmer, P. I.: How sensitive is tropospheric oxidation to anthropogenic emissions?, *Geophys. Res. Lett.*, 35, doi:10.1029/2008GL035718, l22802, 2008.
- 845 Zeng, G., Pyle, J. A., and Young, P. J.: Impact of climate change on tropospheric ozone and its global budgets, *Atmos. Chem. Phys.*, 8, 369–387, doi:10.5194/acp-8-369-2008, 2008.
- Zeng, G., Morgenstern, O., Braesicke, P., and Pyle, J. A.: Impact of stratospheric ozone recovery on tropospheric ozone and its budget, *Geophys. Res. Lett.*, 37, doi:10.1029/2010GL042812, l09805, 2010.
- 850 Zeng, G., Wood, S. W., Morgenstern, O., Jones, N. B., Robinson, J., and Smale, D.: Trends and variations in CO, C<sub>2</sub>H<sub>6</sub>, and HCN in the Southern Hemisphere point to the declining anthropogenic emissions of CO and C<sub>2</sub>H<sub>6</sub>, *Atmos. Chem. Phys.*, 12, 7543–7555, <http://dx.doi.org/10.1029/2012JD018382>, 2012.

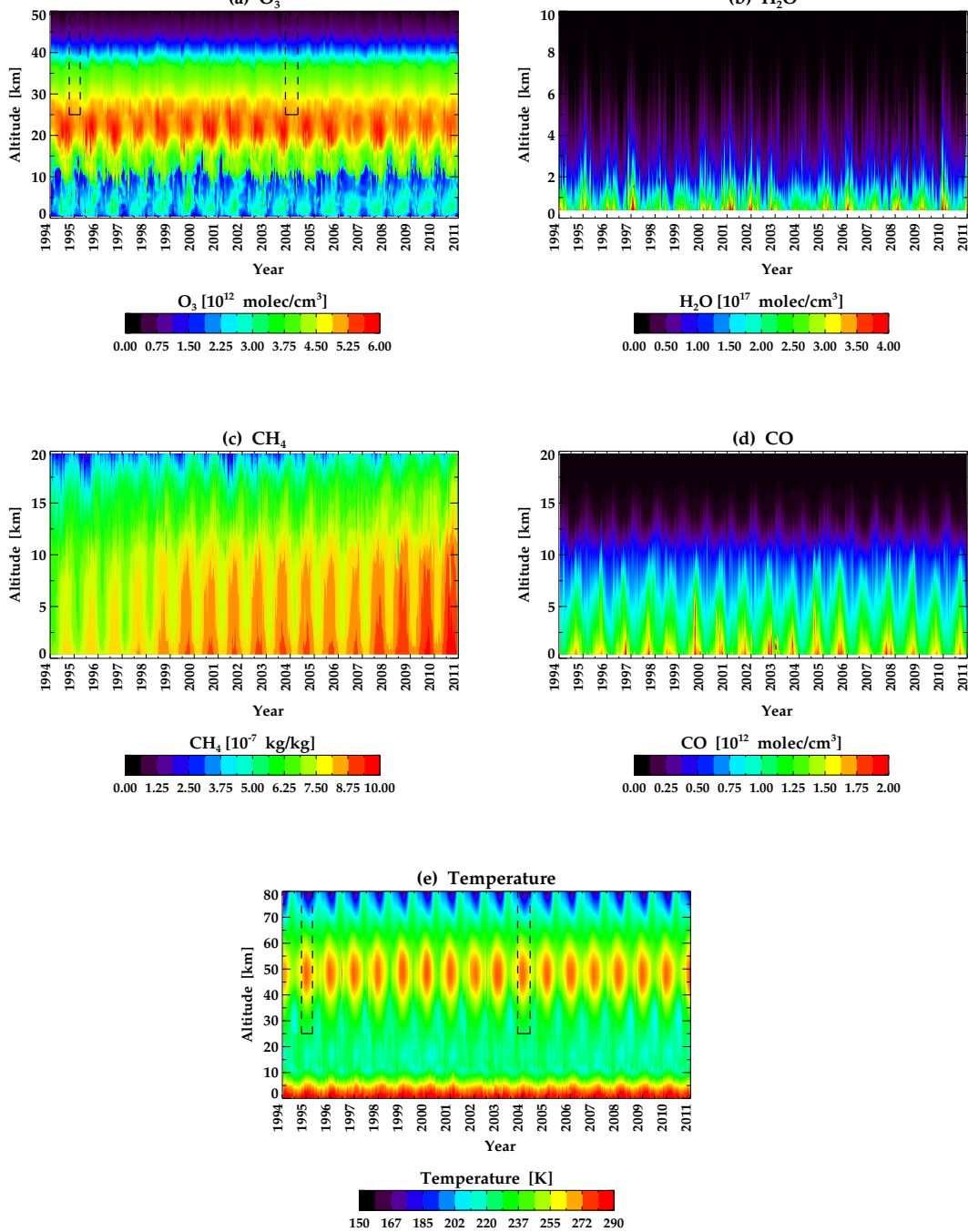


**Figure 1.** (a) Time series of  $O_3$  profiles constructed by ozonesonde measurements spliced with MOPII measurements. (b) Time series of  $H_2O$  profiles constructed by radiosonde measurements spliced with NIWA-UKCA  $H_2O$  (time series of ERAI – NIWA-UKCA  $H_2O$  is not displayed here). (c) Time series of  $CH_4$  profiles constructed by rescaling the NIWA-UKCA  $CH_4$  to surface  $CH_4$  measurements from Cape Grim (Tasmania). (d) Time series of  $CO$  profiles constructed by rescaling the NIWA-UKCA  $CO$  to  $CO$  measurements from the FTIR spectrometer. (e) Time series of temperature profiles constructed by radiosonde measurements (up to 25 km) merged with NCEP/NCAR reanalyses up to the stratopause (50 km) and a mesospheric climatology based on local LIDAR measurements. Above 25 km these data are as used in the retrieval of  $O_3$  from MOPII measurements. The areas within black boxes were filled using a Fourier series gap filling method.

Forcings	Data used
O <sub>3</sub>	<ol style="list-style-type: none"> <li>1. Kinetics effect: O<sub>3</sub> changes → ozonesondes (0-25 km) + MOPII (26-84 km) NIWA-UKCA data for other species and temperature</li> <li>2. Photolysis effect: <math>j_{O^1D}</math> changes according to O<sub>3</sub> changes NIWA-UKCA data for all species and temperature</li> <li>3. Kinetics + photolysis effects: O<sub>3</sub> changes → ozonesondes + MOPII <math>j_{O^1D}</math> changes according to O<sub>3</sub> changes NIWA-UKCA data for other species and temperature</li> </ol>
H <sub>2</sub> O	<ol style="list-style-type: none"> <li>1. Changes in H<sub>2</sub>O → radiosondes (0-8 km) + NIWA-UKCA H<sub>2</sub>O (9-84 km) NIWA-UKCA data for other species and temperature</li> <li>2. Changes in H<sub>2</sub>O → ERAI (0-8 km) + NIWA-UKCA H<sub>2</sub>O (9-84 km) NIWA-UKCA data for other species and temperature.</li> </ol>
CH <sub>4</sub>	Changes in CH <sub>4</sub> → rescaled NIWA-UKCA CH <sub>4</sub> to Cape Grim surface CH <sub>4</sub> NIWA-UKCA data for other species and temperature.
CO	Changes in CO → rescaled NIWA-UKCA CO profiles to FTIR CO NIWA-UKCA data for other species and temperature
T	<p style="text-align: right;">radiosondes (<b>surface-25 km</b>) +</p> <ol style="list-style-type: none"> <li>1. Kinetics effect: temperature changes → <b>NCEP/NCAR reanalyses (26-50 km) + LIDAR climatology (50-84 km)</b> NIWA-UKCA data for all species</li> <li>2. Photolysis effect: <math>j_{O^1D}</math> changes according to temperature changes NIWA-UKCA data for all species and temperature <p style="text-align: right;">radiosondes (<b>surface-25 km</b>) +</p></li> <li>3. Kinetics + photolysis effects: temperature changes → <b>NCEP/NCAR (26-50 km) + LIDAR climatology (50-84 km)</b> <math>j_{O^1D}</math> changes according to temperature changes NIWA-UKCA data for all species</li> </ol>
O <sub>3</sub> , H <sub>2</sub> O, CH <sub>4</sub> , CO, T	Changes in O <sub>3</sub> , H <sub>2</sub> O, CH <sub>4</sub> , CO, and temperature using observations mentioned above. For H <sub>2</sub> O, radiosonde (0-8 km) + NIWA-UKCA (9-84 km) data are used.
Reference	NIWA-UKCA data for all species and temperature

**Table 1. Sensitivity** Simulations performed with the SCM to assess the contribution of changes in the key forcings to OH chemistry at Lauder under clear-sky conditions. The table includes the type of measurement/data set used to prescribe the key forcings. The time period of simulation is between 1994 and 2010.

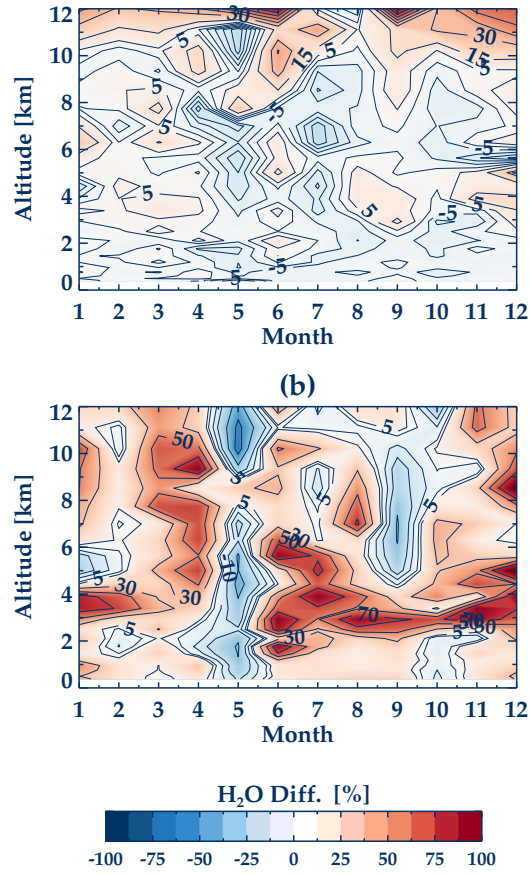


**Figure 2. (a) Multi-annual and monthly mean percentage differences between radiosonde and FPH H<sub>2</sub>O measurements. (b) Multi-annual and monthly-mean percentage differences between NIWA-UKCA output and FPH H<sub>2</sub>O.**

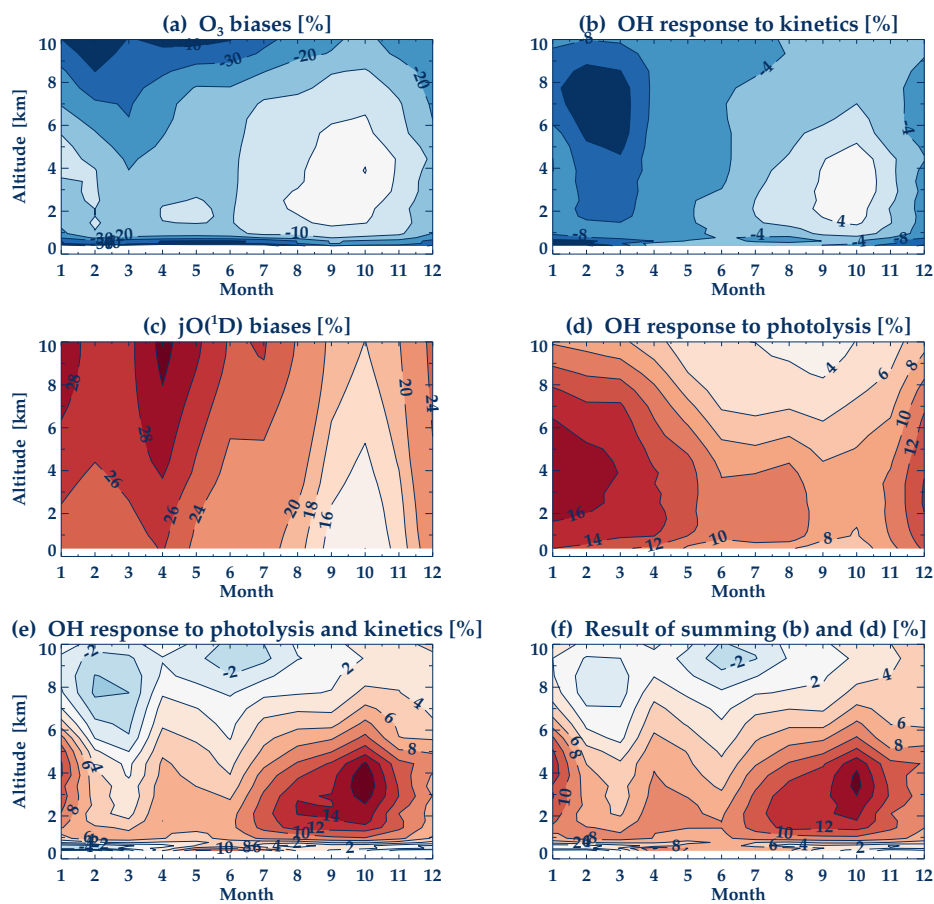


**Figure 3.** Multi-annual and monthly-mean OH responses to O<sub>3</sub> biases between observations and the reference simulation. (a) Difference in O<sub>3</sub> (%) **between ozone sonde and NIWA-UKCA ozone**, relative to **NIWA-UKCA ozone as prescribed** in the reference simulation. (b) OH difference (%) relative to the reference simulation accounting only for the kinetics effects of O<sub>3</sub> differences (e.g. with  $jO(^1D)$  unchanged). (c) Difference in  $jO(^1D)$  (%) relative to the reference simulation. (d) OH difference (%) relative to the reference simulation accounting only for  $jO(^1D)$  differences (e.g. with O<sub>3</sub> unchanged). (e) OH differences relative to the reference simulation considering the combined kinetics and photolysis effects. (f) Sum of (b) and (d).

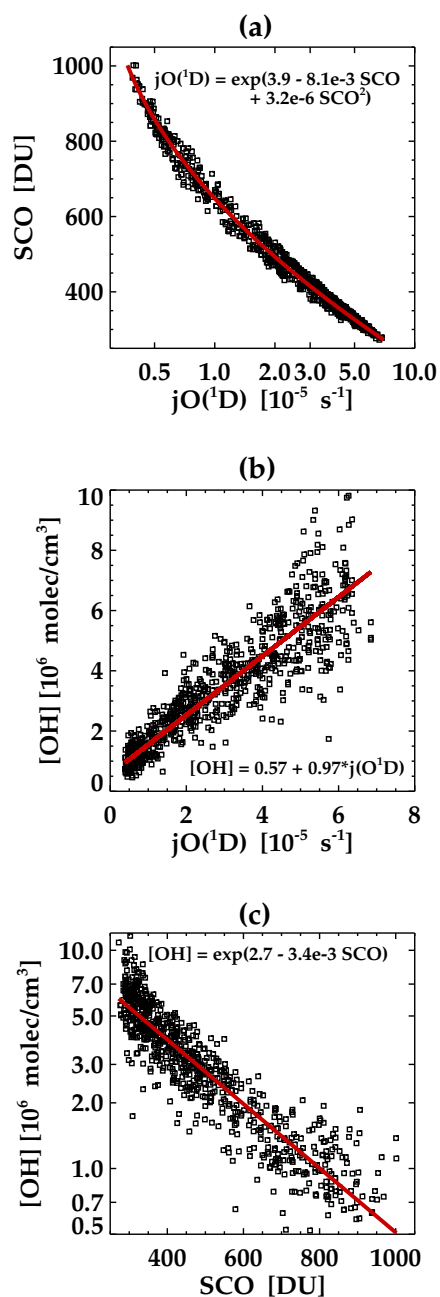


**Figure 4.** (a) Scatter plot of the approximately exponential relationship of  $jO(^1D)$  with the slant column of  $O_3$  (SCO) at 6 km of altitude. (b) Linear relationship of Same, but for  $jO(^1D)$  and OH concentration. The red solid line denotes the linear fit between them. (c) Exponential relationship of the Same, but for the SCO with the and OH concentration. The results shown in this figure are those obtained from the combined simulation (kinetics and photolysis effects). Red lines denote least-squares fits between the variable pairs. The best fits are stated in the panels, with [OH] in units of  $10^6 \text{ molec/cm}^3$ ,  $j_{O^1D}$  in units of  $10^{-5} \text{ s}^{-1}$ , and the SCO in Dobson Units.

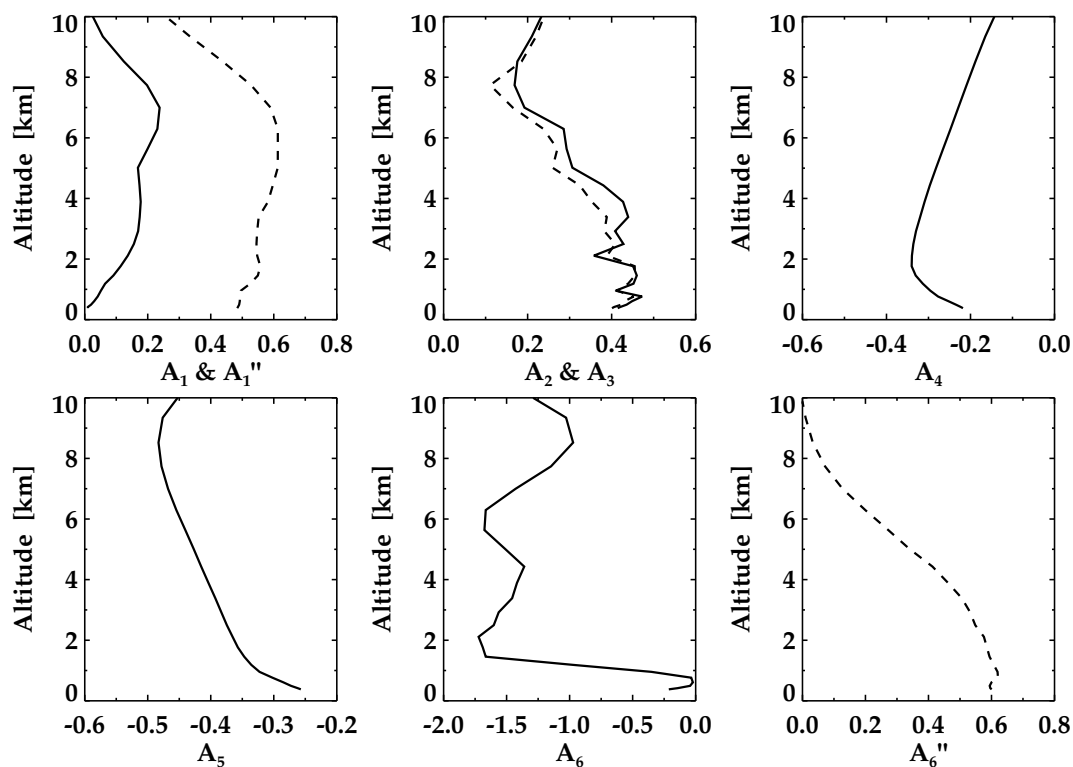


**Figure 5.** Sensitivity coefficients ‘ $A_i$ ’ between OH and each perturbation variable: In the calculation, multi-annual mean relative differences in OH and in the forcing are ratioed. (a) Sensitivity of OH to changes in  $O_3$  levels (kinetics effect) denoted by  $A_1$  (solid line) and to changes in  $jO(^1D)$  due to changes in  $O_3$  (photolysis effect) denoted by  $A_1''$  (dashed line); (b) sensitivity of OH to changes in radiosonde – NIWA-UKCA CCM  $H_2O$  ( $A_2$  solid line) and to changes in ERAI – NIWA-UKCA  $H_2O$  ( $A_3$  dashed line); (c) sensitivity of OH to changes in  $CH_4$  ( $A_4$ ); (d) sensitivity of OH to changes in CO ( $A_5$ ); (e) sensitivity of OH to changes in temperature (kinetics effect) denoted by  $A_6$ ; (f) sensitivity of OH to changes in  $jO(^1D)$  due to changes in temperature (photolysis effect) denoted by  $A_6''$ .

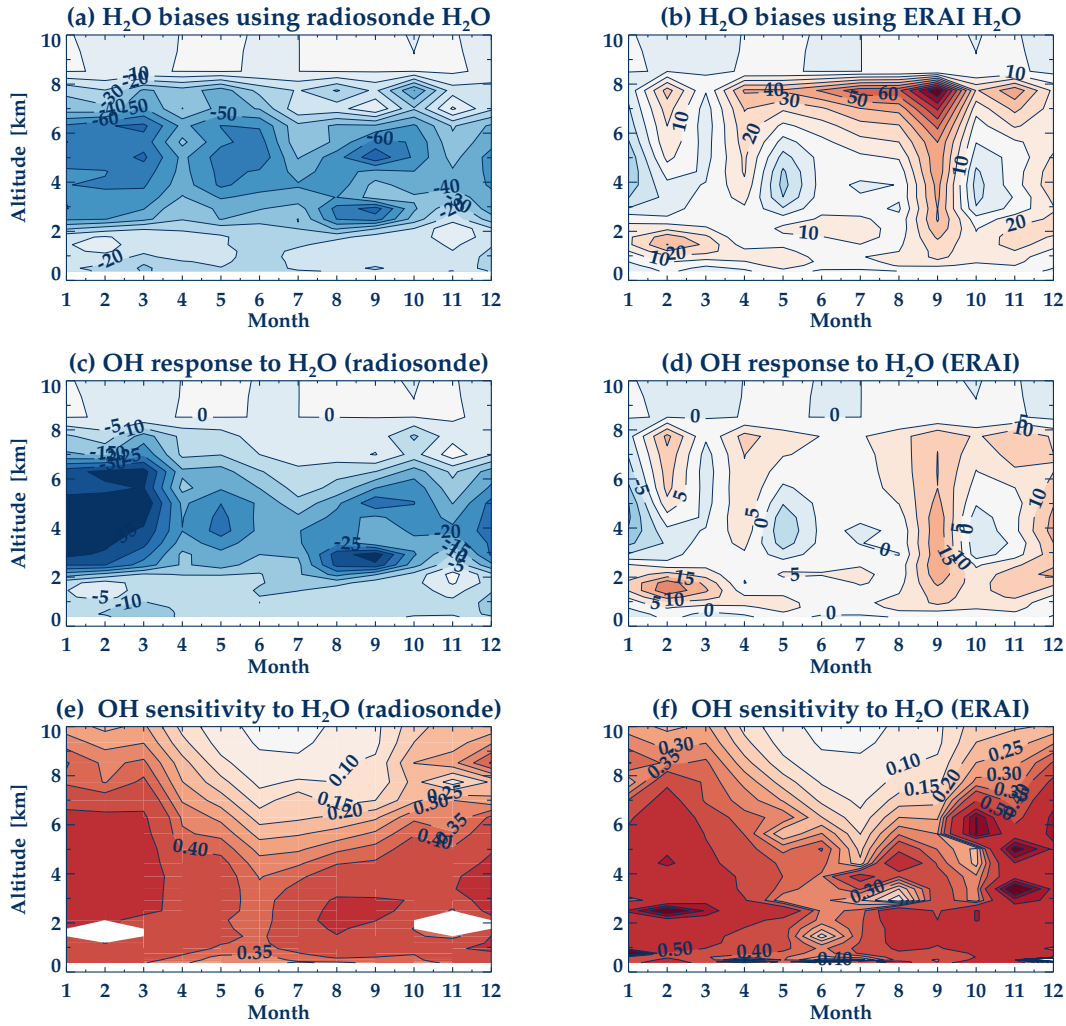


**Figure 6.** Multi-annual and monthly-mean OH responses to H<sub>2</sub>O between perturbation simulations and the reference simulation. (a) Difference in Radiosonde – NIWA-UKCA H<sub>2</sub>O (%) relative to the reference simulation. (b) Difference in ERAI – NIWA-UKCA H<sub>2</sub>O (%) relative to the reference simulation. (c) OH difference (%) relative to the reference simulation **between simulations using radiosonde and NIWA-UKCA H<sub>2</sub>O (panel a)**. (d) OH differences (%) relative to the reference simulation **between simulations using ERAI and NIWA-UKCA CCM H<sub>2</sub>O (panel b)**. (e) Ratio of relative OH changes (panel c) to relative changes in H<sub>2</sub>O (panel a). (f) Ratio of relative OH changes (panel d) to changes in H<sub>2</sub>O (panel b). Above 8 km NIWA-UKCA H<sub>2</sub>O was used in both cases. Therefore, differences with respect to the reference simulation are close to 0.

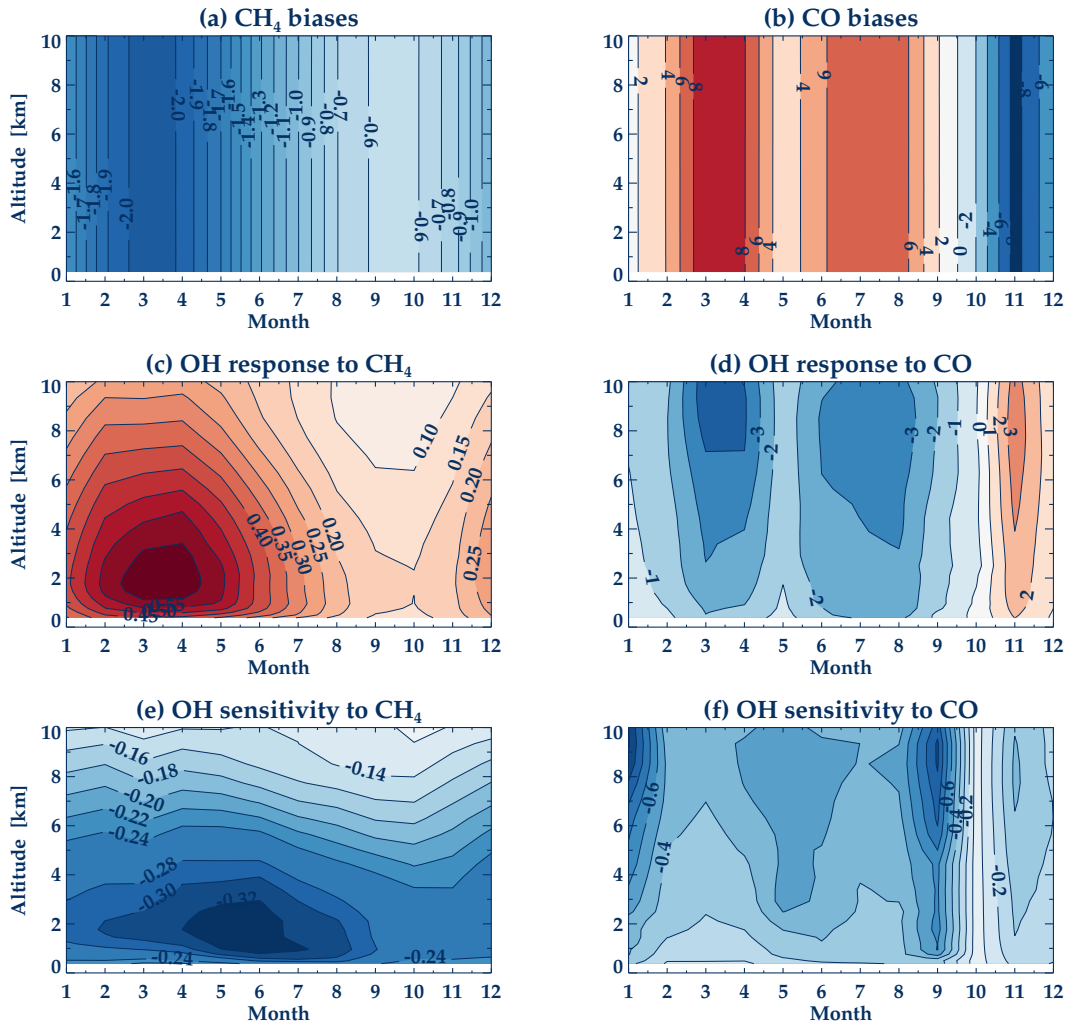


**Figure 7.** Multi-annual and monthly-mean OH responses to CH<sub>4</sub> and CO biases between observations and the reference simulation. (a) Difference in CH<sub>4</sub> (%) relative to the reference simulation. (b) Difference in CO (%) relative to the reference simulation. (c) OH difference (%) relative to the reference simulation caused by the CH<sub>4</sub> change (panel a). (d) OH difference (%) relative to the reference simulation caused by the CO change (panel b). (e) Ratio of relative OH changes (panel c) to relative changes in CH<sub>4</sub> (panel a). (f) Ratio of relative OH changes (panel d) to relative changes in CO (panel b).

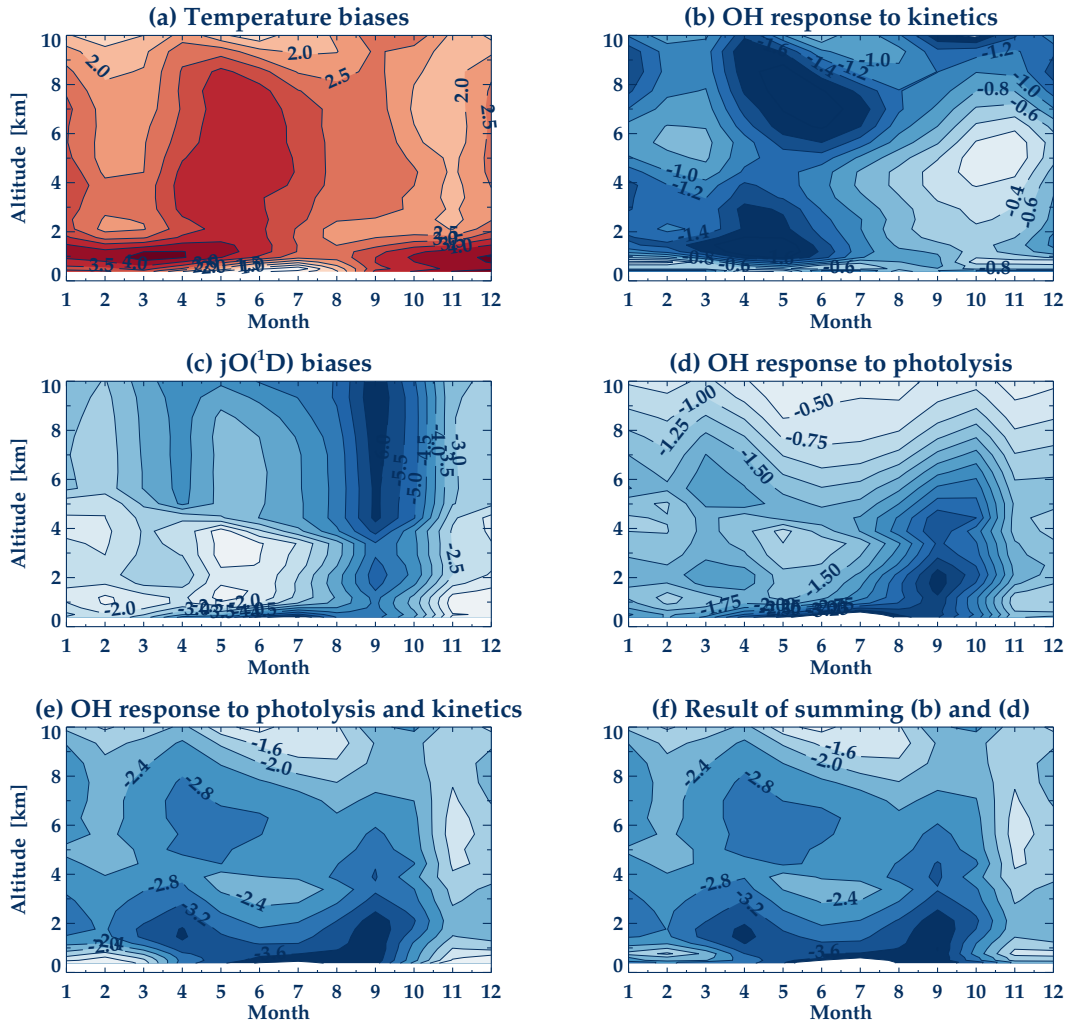


**Figure 8.** Multiannual and monthly-mean OH responses to temperature biases between observations (radiosonde and **NCEP/NCAR** temperature) and the reference simulation. (a) Difference in radiosonde and **NCEP/NCAR** temperature (K) relative to the reference temperature. (b) OH difference (%) relative to the reference simulation accounting only for the kinetics effects of temperature differences (e.g. with  $jO(^1D)$  unchanged). (c) Difference in  $jO(^1D)$  (%) relative to the reference simulation. (d) OH difference (%) relative to the reference simulation accounting only for  $jO(^1D)$  differences (i.e. with temperature unchanged). (e) OH differences relative to the reference simulation considering the combined kinetics and photolysis effects. (f) Sum of (b) and (d).

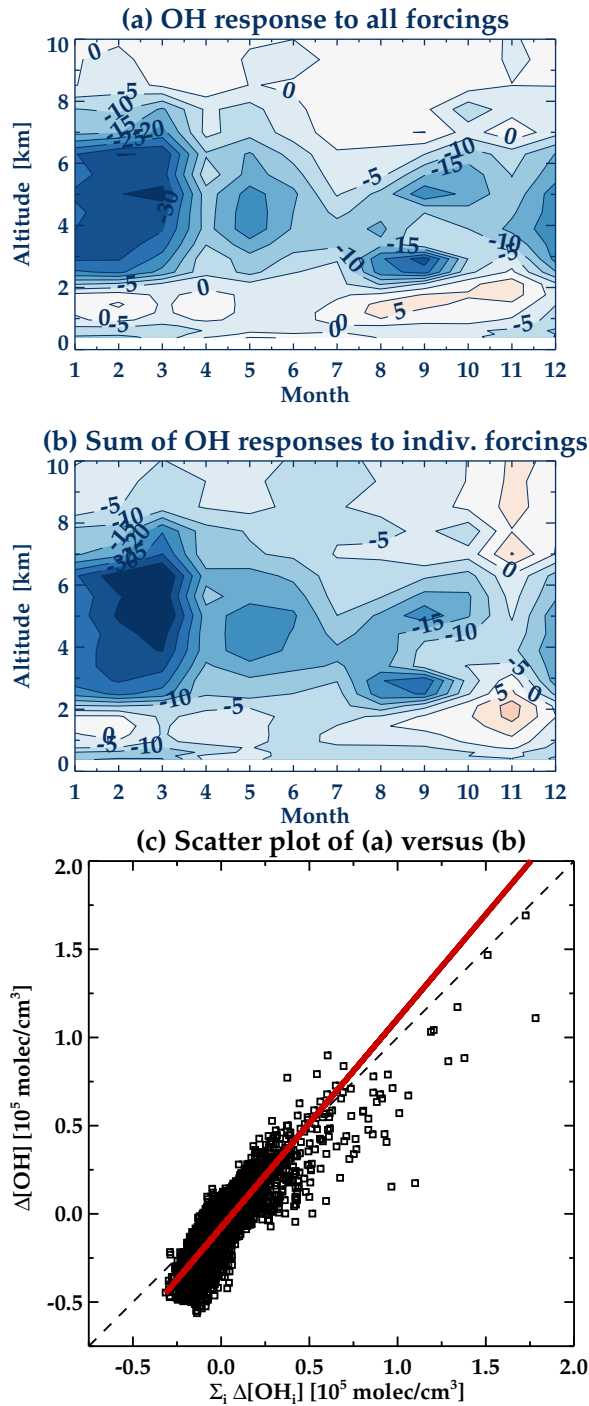


**Figure 9.** (a) Multi–annual and monthly–mean percentage difference in OH between a simulation with bias–correction applied to all five fields and the reference simulation. Radiosonde H<sub>2</sub>O is assumed below 8 km. (b) Summation of all the single forcing contributions as expressed by the right hand side of Eq. (4). Radiosonde H<sub>2</sub>O is assumed below 8 km. (c) Scatter plot of the response of OH to the combination of all forcings (vertical axis, denotes as  $\Delta[\text{OH}]$ ) versus the summation of the OH response to individual forcings (horizontal axis) as expressed by the right hand side of Eq. (4) (denoted by  $\sum_i \Delta[\text{OH}_i]$ ). **The red solid line denotes an orthogonal fit. The black dashed line is the diagonal.**

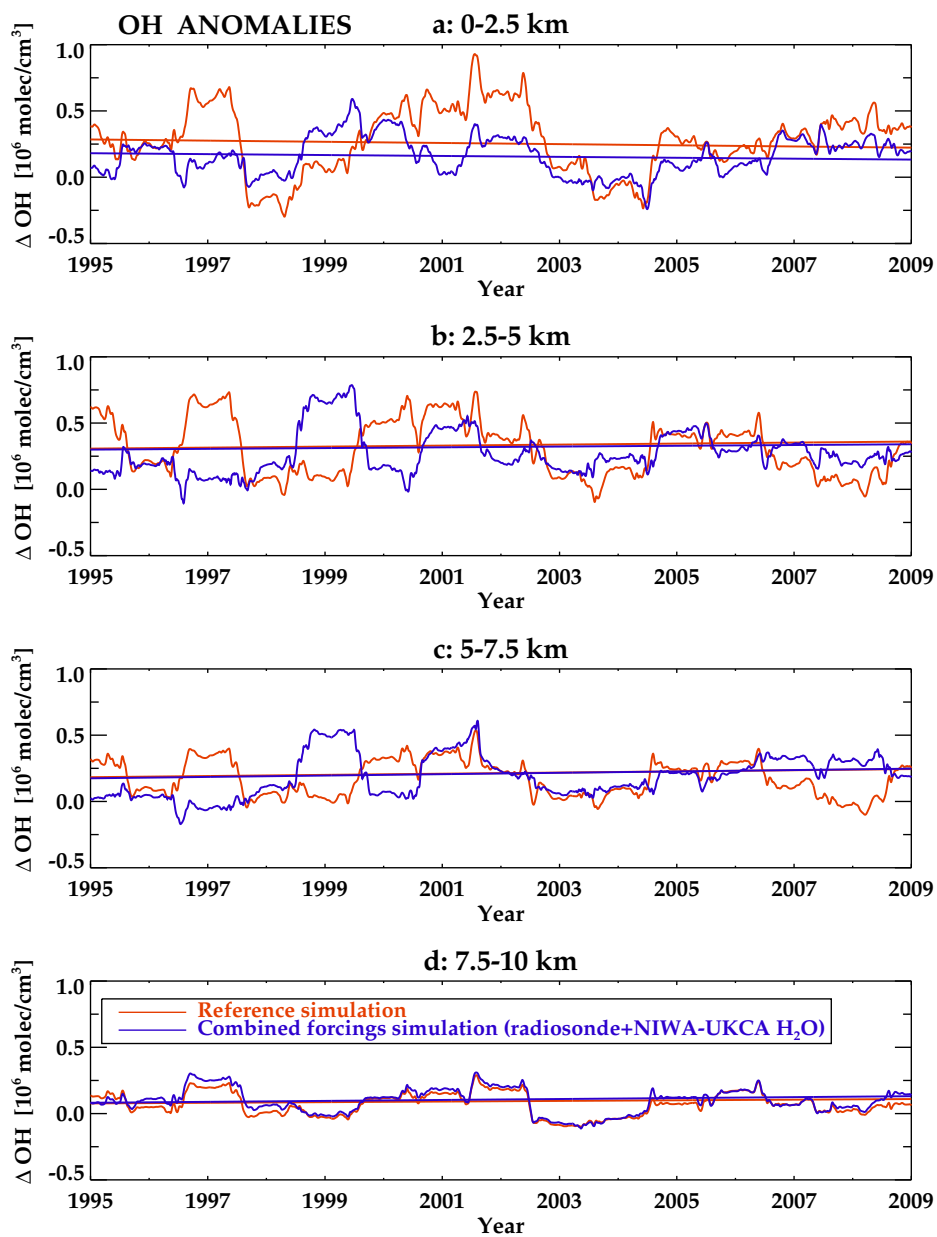


**Figure 10.** Variability and trends of the OH anomalies at different altitudes: (a) 0-2.5 km, (b) 2.5-5 km, (c) 5-7.5 km, and (d) 7.5-10 km. The red solid line is the time series of the reference simulation and the blue solid line is the combined forcings simulation considering radiosonde – NIWA-UKCA H<sub>2</sub>O.

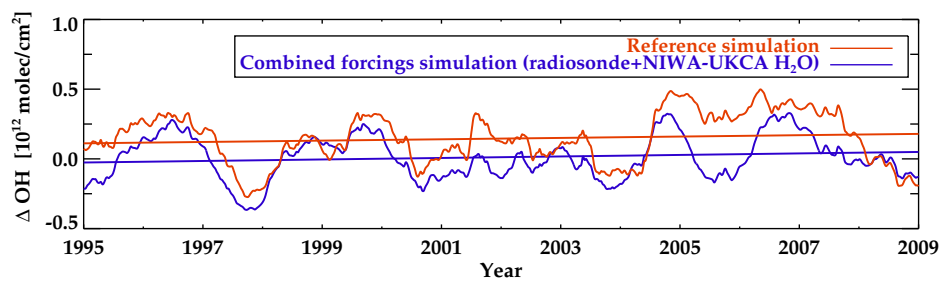


**Figure 11.** Variability and trend of the OH column anomaly. The red solid line is the time series of the reference simulation and the blue solid line is the combined forcings simulation considering radiosonde – NIWA-UKCA H<sub>2</sub>O.

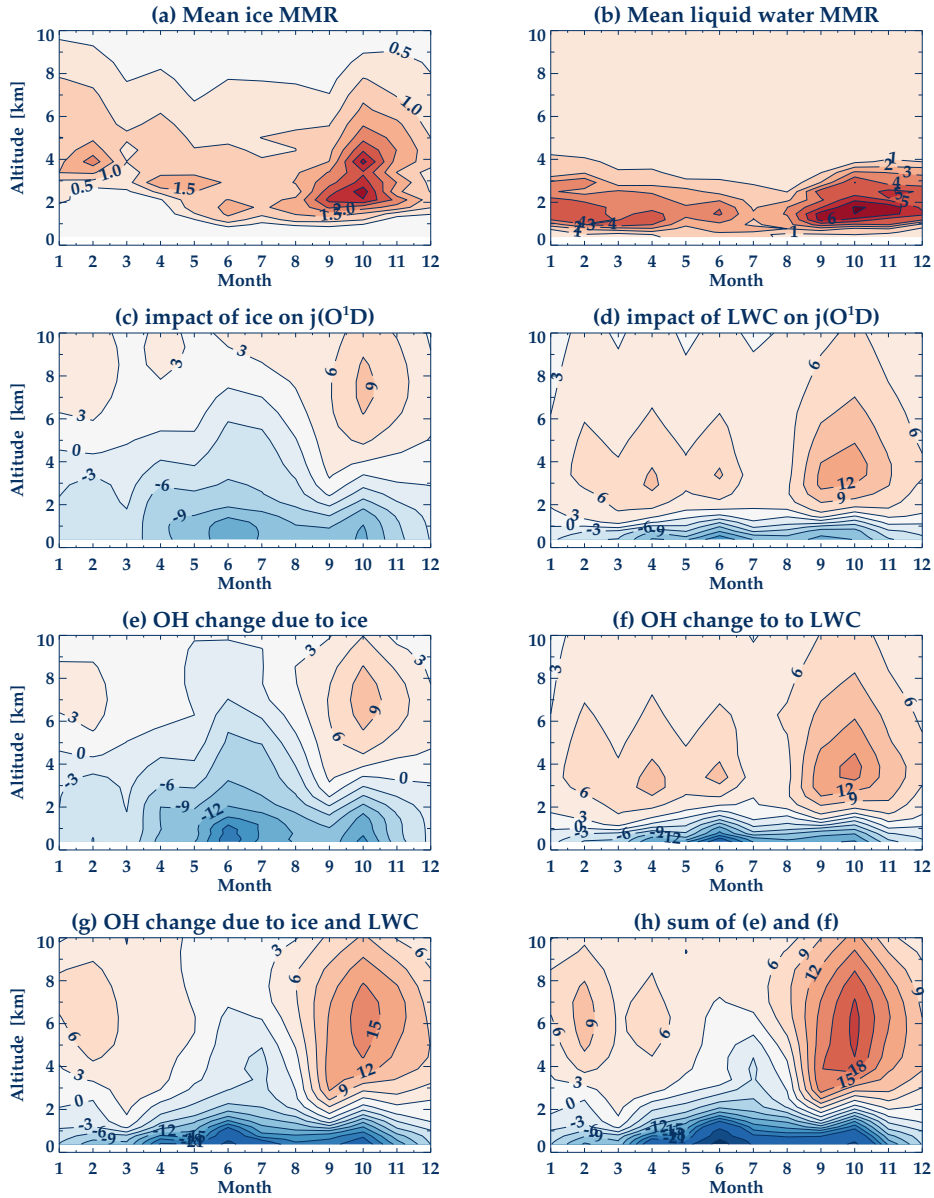


**Figure 12.** Multi-annual and monthly-mean OH responses to the presence of clouds. Multi-annual and monthly mean (a) ice content ( $10^{-5}$  kg/kg). (b) liquid water content ( $10^{-5}$  kg/kg). (c) Response of  $j_{O^1D}$  (%) to the presence of ICs relative to the cloud-free reference simulation. (d) response of  $j_{O^1D}$  (%) to the presence of LWCs relative to the cloud-free reference simulation. (e) response of OH (%) to the presence of ICs relative to the cloud-free reference simulation. (f) Response of OH (%) to the presence of LWCs relative to the cloud-free reference simulation. (g) response of OH (%) to the presence of both LWCs and ICs relative to the cloud-free reference simulation. (h) Sum of 3a and 3b.